CATARINA MARTINS RAPOSO

STUDY OF THE TRIB2 PROTEIN NETWORK

UNIVERSIDADE DO ALGARVE

Departamento de Ciências Biomédicas e Medicina

2018

CATARINA MARTINS RAPOSO

STUDY OF THE TRIB2 PROTEIN NETWORK

Master in Oncobiology – Molecular Mechanisms of Cancer

This work was done under the supervision of

Bibiana Ferreira, Ph.D

Wolfgang Link, Ph.D

UNIVERSIDADE DO ALGARVE

Departamento de Ciências Biomédicas e Medicina

2018

STUDY OF THE TRIB2 PROTEIN NETWORK

Declaração de autoria de trabalho

Declaro ser a única autora deste trabalho que é original e inédito. Autores e trabalhos consultados estão devidamente citados no texto e constam da listagem de referências incluída.

Catarina Martins Raposo

Copyright © 2018 Catarina Martins Raposo

A Universidade do Algarve reserva para si o direito, em conformidade com o disposto no Código do Direito de Autor e dos Direitos Conexos, de arquivar, reproduzir e publicar a obra, independentemente do meio utilizado, bem como de a divulgar através de repositórios científicos e de admitir a sua cópia e distribuição para fins meramente educacionais ou de investigação e não comerciais, conquanto seja dado o devido crédito ao autor e editor respetivos.

Agradecimentos

A realização desta dissertação de mestrado contou com diferentes apoios e incentivos sem os quais não teria sido possível concretizá-la. Passo a citá-los abaixo.

Agradeço ao professor doutor Wolfgang Link por me ter recebido no seu laboratório e por toda a ajuda que, tão prontamente, sempre me deu. Pelo total apoio e disponibilidade.

Agradeço à Bibiana por todos os ensinamentos e conselhos. Pelas opiniões e críticas. Pelas palavras de incentivo nos momentos menos felizes.

Agradeço à Rita por toda a paciência. Por ouvir os meus desabafos e dar os melhores conselhos do mundo.

Agradeço ao André. Pelo companheirismo, força e apoio nos instantes mais difíceis. Por tudo.

Agradeço à Catarina Martins e ao André Fonseca. Agradeço à Susana Machado e ao João Santos. Agradeço ao Leonardo. Agradeço-vos por tornarem este ano mais leve. Sem vocês teria sido muito mais difícil.

E por fim, agradeço muito aos meus pais. Sem eles este projeto não teria sido possível. Pelo apoio incondicional, incentivo e amizade. A eles dedico este trabalho!

Abstract

Melanoma is a highly aggressive type of cancer that arises from the transformation of melanocytes, the pigment-producing cells of the human skin. Metastatic melanoma is the deadliest form of skin cancer for which recently two treatment options have improved clinical outcome: targeted therapies and immunotherapy. However, the majority of patients primarily fail to respond or develop resistance to these drugs. The Link lab has discovered a novel mechanism of drug resistance facilitated by the oncoprotein TRIB2 via its direct interaction with AKT and consequently, AKT activation and AKT-dependent inactivation of FOXO and p53. Intriguingly, the tumor suppressor TRIB3 exerts the opposite effect on AKT. Therefore, we hypothesized that TRIB2 and TRIB3 compete for AKT binding, determining the level of drug resistance. The current study was performed aimed at understanding the mechanism by which TRIB2 and TRIB3 exert opposing effects on AKT. We used protein complementation assays and immunoprecipitation assays to characterize this mechanism.

Our results show that TRIB3 is able to disrupt the association between TRIB2 and AKT thus contributing to decrease the phosphorylation of the Serine 473 on AKT and preventing cell tumorigenesis. These findings are in concordance with literature describing TRIB3 as a tumour suppressor.

Our data also demonstrate that increasing amounts of TRIB2 stabilize the association between TRIB3 and AKT. One possibility that might explain these observations is that in a cellular system with low levels of TRIB3, TRIB2 is able to bind and promote AKT activation. In a system with high levels of TRIB3, AKT preferentially interacts with TRIB3, preventing Serine 473 AKT phosphorylation. Therefore, we suggest that AKT has higher binding affinity to TRIB3 than to TRIB2.

Understanding the resistance mechanism caused by TRIB2 and the role of TRIB3 in preventing this mechanism is key to develop new and better therapies for patients with melanoma.

Resumo

O melanoma é uma forma muito agressiva de cancro de pele que deriva da transformação maligna dos melanócitos - as células responsáveis pela produção de melanina que se encontram na camada basal da epiderme da pele humana. Apesar de representar apenas 5% de todos os tipos de cancro, o melanoma é responsável pela morte de 80% dos pacientes com cancro de pele. Para além disso, a incidência deste tipo de cancro tem aumentado muito nas últimas três décadas e a sua mortalidade aumenta de forma mais rápida do que qualquer outro tipo de cancro.

Análises genéticas mostram que existem duas vias de sinalização frequente e comummente mutadas em tecido cutâneo de melanoma: a via MAPK e a via PI3K/AKT. Assim sendo, a alteração destas vias é importante no desenvolvimento e progressão deste tipo de cancro de pele, tendo como consequências o aumento da proliferação celular e também a resistência a fármacos que tenham como alvo proteínas presentes em qualquer uma destas vias de sinalização.

Até há pouco tempo, o tratamento do melanoma metastático era realizado através de elevadas doses de interleucina-2 ou dacarbazina - dois fármacos quimioterapêuticos com taxas de sucesso que não superam os 20% e efeitos secundários muito severos. Nos últimos anos surgiram duas abordagens terapêuticas que se mostraram mais eficientes no tratamento do melanoma: as terapias dirigidas a membros da via MAPK (como o BRAF e o MEK) e também a imunoterapia que passa pela inibição de proteínas que controlam os checkpoints imunitários (como CTLA4, PD-1 e PD-L1). Embora estas abordagens se tenham mostrado mais eficientes no tratamento do melanoma metastático do que as anteriores, a maioria dos pacientes continua a não responder ou adquire resistência a estes tratamentos. Assim sendo, investigar a causa destes mecanismos de resistência é um passo muito importante para o desenvolvimento de terapêuticas novas mais eficazes.

Recentemente, o nosso grupo descobriu um novo mecanismo de resistência a uma série de medicamentos utilizados em ensaios clínicos ou já autorizados e prescritos para o tratamento do melanoma. Este mecanismo é mediado pela proteína TRIB2. TRIB2 codifica um dos três membros da família das proteínas pseudocinases tribbles. O nosso grupo identificou TRIB2 como um oncogene no contexto de melanoma e publicou dados importantes que mostram que, quer *in vitro* quer *in vivo*, a alta expressão de TRIB2 confere resistência a inibidores da via PI3K/mTOR e também a vários fármacos quimioterapêuticos como a dacarbazina. Para além disso a alta expressão de TRIB2 também confere resistência a inibidores de MEK e inibidores de imunocheckpoint.

Mecanisticamente, o nosso grupo mostrou recentemente que TRIB2 promove a ativação de AKT, aumentando a fosforilação da serina 473 do AKT por mTORC2, via interação proteína-proteína. Esta ativação leva à inibição do supressor tumoral FOXO e ao aumento da atividade de MDM2, responsável por degradar o p53. Assim, a expressão dos genes alvo de FOXO e p53, que levariam à apoptose das células tumorais, está diminuída pelo aumento de TRIB2.

Surpreendentemente, um grupo em Espanha com o qual mantemos uma estreita colaboração, liderado por Guillermo Velasco, demonstrou há bem pouco tempo que outro membro da família tribbles, TRIB3, parece ter o efeito oposto na ativação de AKT. O grupo sugere que TRIB3 funciona como um supressor tumoral e que a sua inativação leva a um aumento da tumorigénese.

Uma vez que TRIB2 e TRIB3 parecem ter efeitos opostos na progressão das células tumorais, tendo funções contrárias na via de sinalização PI3K/AKT, então, o balanço da expressão de TRIB2 e TRIB3 é um fator importante na patogénese do melanoma e na resposta destes doentes à terapia. Assim sendo, a nossa hipótese é que TRIB2 e TRIB3 competem pela ligação a AKT. Para testar esta hipótese utilizámos o método PCA (Protein Complementation Assay) e ensaios de co-imunoprecipitação.

Os nossos resultados de PCA mostram que o aumento de TRIB3 causa uma diminuição na associação entre TRIB2 e AKT na linha celular HEK293T, sugerindo assim que TRIB3 é capaz de perturbar a associação entre TRIB2 e AKT. Os nossos dados sugerem que, ao interferir na ligação TRIB2-AKT, TRIB3 inibe a fosforilação da Serina 473 do AKT (facilitada por TRIB2), prevenindo a sua ativação e evitando a malignidade das células. Este facto vai de encontro ao descrito em estudos anteriores sobre a função supressora tumoral de TRIB3. Este nosso projeto mostra assim, pela primeira vez, que os membros da família tribbles competem pela ligação a AKT.

Por outro lado, ao contrário do que estávamos à espera, as nossas experiências de PCA mostram ainda que TRIB2 estabiliza a interação entre TRIB3 e AKT. Apesar de não existirem estudos na literatura acerca deste tópico, uma possibilidade que explique este facto é que, apenas em células que expressem pouco TRIB3, TRIB2 é capaz de ativar AKT. Em células com elevada expressão de TRIB3, o AKT liga-se preferencialmente a TRIB3, mantendo-se inativo. Estas experiências sugerem assim que a afinidade de ligação de AKT é consideravelmente maior por TRIB3 do que por TRIB2.

Tentámos perceber, usando a técnica de *western blot*, se a diminuição da interação entre TRIB2 e AKT se refletiria, de facto, numa diminuição da fosforilação da Serina 473 do AKT mas os resultados foram inconclusivos devido a uma desigualdade no controlo de carga utilizado. Pensamos que este facto se deveu à grande quantidade de DNA transfetado para as células. Apesar disso, as únicas bandas comparáveis, parecem mostrar que células transfetadas com maior quantidade de TRIB3 têm menos ativação de AKT, o que vai de encontro aos resultados anteriores.

Para ultrapassar este problema técnico decidimos utilizar a linha HEK293T, gerada anteriormente no nosso laboratório, que expressa estavelmente TRIB2 para podermos diminuir a quantidade de DNA a ser transfetada nestas células. Tentámos validar os resultados do PCA utilizando co-imunoprecipitação nesta linha celular mas os resultados mostraram-se, mais uma vez, inconclusivos devido à falha de um controlo utilizado na experiência.

Para, no futuro, validar esta hipótese num sistema mais representativo de melanoma, ou seja, em células onde normalmente exista a expressão de TRIB2, procedemos à criação de uma linha celular de melanoma: UACC-62 *knock-out* para o gene de TRIB2, utilizando a técnica de CRISPR-Cas9. Obtivemos vários clones de células UACC-62 sem a expressão de TRIB2 que poderão ser comparados com a linha UACC-62 parental.

Em suma, este projeto confirma o anteriormente descrito sobre a função supressora tumoral de TRIB3 e sugere que esta deriva de uma diminuição da interação entre TRIB2 e AKT causada por TRIB3, prevenindo a fosforilação e ativação de AKT. Neste estudo demonstrámos ainda que AKT se liga preferencialmente a TRIB3 em vez de TRIB2.

Sugerimos um estudo aprofundado do mecanismo molecular pelo qual a interação de TRIB2 e AKT é perturbada por TRIB3 tendo em vista um melhor conhecimento do mecanismo de resistência provocado por TRIB2 em pacientes com melanoma.

Table of Contents

1 Introduction 3

1.1 Cancer 3

1.2 Melanoma 4

1.2.1 Clinical Grading System 7

1.2.2 Melanoma genetics 7

1.2.3 PI3K-AKT pathway 8

1.2.4 Melanoma treatment options 9

Melanoma resection 9

Chemotherapy 9

Immunotherapy 10

Targeted therapies 12

1.2.5 Resistance mechanisms 14

Drug inactivation 15

Drug Efflux 15

DNA damage repair 16

Cell death inhibition 16

Epithelial-Mesenchymal Transition and Metastasis 16

1.2.6 Tribbles 16

The role of TRIB2 in melanoma prognosis 18

The role of TRIB3 in cancer 19

1.3 Hypothesis 20

2 Methodology 23

2.1 Cell culture 23

2.1.1 Cell count 23

2.1.2 Cell lines 24

2.2 Western Blot ... 24
  2.2.1 Total protein extraction ... 25
  2.2.2 Total protein quantification ... 25
  2.2.3 SDS-PAGE ... 27
  2.2.4 Protein transfer ... 28
  2.2.5 Blocking step ... 28
  2.2.6 Antibodies incubation ... 29
  2.2.7 Protein detection ... 29
2.3 Protein Complementation Assay ... 30
2.4 PCA Optimization ... 31
2.5 Plasmid amplification ... 32
  2.5.1 Bacterial transformation and plasmid amplification ... 32
  2.5.2 DNA extraction ... 33
2.6 Immunoprecipitation ... 33
2.7 TRIB KO - CRISPR ... 34
3 Results ... 37
3.1 PCA optimization ... 37
3.2 TRIB3 is able to disrupt TRIB2-AKT association ... 40
3.3 TRIB2 stabilizes TRIB3-AKT interaction ... 41
3.4 293T stable cell line expressing TRIB2 ... 44
3.5 UACC-62: TRIB2 KO ... 46
4 Discussion ... 51
5 Conclusion and Future Perspectives ... 57
6 Bibliography ... 61

Figures Index

Figure 1 - The hallmarks of cancer. A normal cell needs to overcome several mechanisms to become transformed. The first described hallmarks were: self-sufficiency in growth signals, insensitivity to anti-growth signals, evading apoptosis, sustained angiogenesis, limitless replicative potential and tissue invasion and metastasis. In 2011 the same authors suggested two more hallmarks involved in tumorigenesis: genomic instability and tumor promoting inflammation. New capabilities have been emerging in the last years: the ability of cancer cells to reprogram its metabolism and to avoid the immune system mediated destruction. Adapted from Hanahan D. and Weinberg R., “The Hallmarks of cancer”, Cell, 2011 [4] ....

Figure 2: **Changes in annual lifetime risk of developing invasive melanoma in the United States from 1930 to 2016.** Adapted from "Analysis of trends in US melanoma incidence and mortality", JAMA Dermatology, 2017 [3]. ....

Figure 3: **Estimated number of annual deaths from melanoma in the United States from 2009 to 2016**. Adapted from "Analysis of trends in US melanoma incidence and mortality", JAMA Dermatology, 2017 [3]. ....

Figure 4 - Cutaneous transformation of melanocytes. The accumulation of genetic changes induced by UV light both in tumor suppressor genes and oncogenes are responsible for the transformation of the pigment producing cells of the human skin. Adapted from Hussein, Mahmoud R., “Ultraviolet radiation and skin cancer: molecular mechanisms”, Journal of Cutaneous Pathology, 2005 [17]. 6

Figure 5 - Stages of melanoma. The first stage is the less aggressive, cell proliferation is limited to the epidermis, not reaching the dermis so the treatment applied in this case in only the surgical resection. Melanomas on stages I and II are characterized by tumor thickness and ulceration and are treated by surgical resection followed by drug or radiation treatment. When cancer cells are already spread to the lymph nodes is stage III and surgical removal of the lymph nodes is required. If cancer has spread into distant organs it is a IV stage melanoma and is treated with chemotherapy [5]. ....

Figure 6 - The PI3K-AKT pathway. Diagram of key activators and regulators of the PI3K-AKT signalling network. Adapted from Davies, Michael A., "The role of the PI3K-AKT Pathway in Melanoma", The Cancer Journal, 2012 [21]. 8

Figure 7 - Signatures of mutational processes in human cancer. Cancer with high mutational load respond better to immunotherapy and tend to be highly resistant to traditional treatments. Adapted from "Signatures of mutational process in human cancer", Nature, August 2013 [38]. 11

Figure 8 - Overview of the MAPK pathway. Activation of a cell surface receptor tyrosine kinase (RTK) leads to a sequential phosphorylation and activation of proteins in the MAPK pathway: RAS, RAF, MEK and ERK. ERK activation mediates phosphorylation of key proteins involved in cellular proliferation and survival. Adapted from [2]. ....

Figure 9 - Resistance mechanisms to cancer therapy. The main mechanisms that can enable or promote direct or indirect drug resistance in human cancer cells include drug inactivation, drug efflux or the ability of cancer cells to increase the DNA damage repair. Adapted from [58]. 15

Figure 10 - Structure of Tribbles family. Tribbles structure has three main domains: a central serine-threonine kinase like domain (resembles a kinase domain but has some aminoacids lacking that are essential to the catalytic activity), a MEK-1 and a COP-1 binding domain. Adapted from [1]. ....

Figure 11 - Tribbles tissue expression. TRIB1 is highly expressed in the bone marrow, peripheral blood leukocytes, thyroid gland and pancreas [76, 77]. TRIB2 is highly expressed in peripheral blood leukocytes, thymus, heart, brain, kidney, lung, skin and white adipose tissue [76, 77]. TRIB3 is more expressed in human liver [76]. 18

Figure 12 - Scheme of the Neubauer Chamber. Despite the fact of the recent technical development of scientific laboratories, the Neubauer chamber remains the most common method used for cell counting around the world. ....

Figure 13 – BSA standard curve concentrations To determine the protein concentration of our test samples we used a linear standard curve. Serial dilutions were obtained from a BSA stock solution at 2000 µg/µL. Letters **A** to **G** refer to seven different BSA concentrations where A (2 mg/mL BSA), B (1.25 mg/mL BSA), C (0.75 mg/mL BSA), D (0.75 mg/mL), E (0.375 mg/Ml BSA), F (0.185 mg/mL BSA) and G (0 mg (mL BSA). All dilutions were obtained using H_2O ....

Figure 14 - Differently sized proteins migrate in different speeds across the gel. When the voltage is applied, the negative charged molecules migrate through the gel in direction to the positive pole. The small proteins in our samples migrate easily and the larger proteins are more likely to be retained (migrating less).. 27

Figure 15 - Separation ranges of proteins in SDS-PAGE. The percentage of acrylamide present in the gel determine the speed of migration and the degree of separation between the proteins. 28

Figure 16 - Scheme of the PCA structural associations. PCA is a structural complementation assay designed for PPIs studies. The system is composed of two subunits, Large BiT (LgBiT; 18kDa) and Small BiT (SmBiT; 11 amino acid peptide) that are expressed as fusions to target proteins of interest. If these two proteins do interact the split fragment of luciferase will come together and give off a luminescence signal in the presence of an added substrate Promega Nano-Glo Live Cell Assay system (#N2011)... 30

Figure 17 - Possible constructs of TRIB2 and AKT. There are four possible fusions of the protein of interest to the luciferase fragment. Each protein of interest can be cloned next to a Small or Large luciferase fragment or fused to either its C' or N' terminal region. ....

Figure 18 - **Presence of tribble members in melanoma and non-melanoma cell lines. A)** Western blot showing protein levels of Tribble family members in melanoma cell lines SK-MEL28, G361 and A375 and non-melanoma cell lines 293T and U2OS. Protein levels were assessed with Tribble specific antibodies. Tubulin was used as a loading control. 20 µg total protein loaded per lane and separated by 10% SDS-PAGE. **B)**. Tribble members (TRIB1, TRIB2 and TRIB3) mRNA levels of melanoma A375, G361 and SK-MEL28 and non melanoma cell lines 293T and U2OS. mRNA expression levels were evaluated using RT-PCR and data was analysed using Bio-Rad CFX manager 3.1 software.....................

Figure 19 - PCA optimization. PCA is based on the interaction of two luciferase fragments, a small one (represented by 1.1) and a large one (represented by 2.1). Each one of these fragments can be fused to AKT or to TRIB2 in their amino (N) or carboxyl termination (C). We transiently transfected 293T cells for 24 hours using different pairs of constructs. At the end point we added the luciferase substrate for 5 minutes and acquired the luminescence signal. As negative control we used non-transfected cells (Untransfected) and cells transfected with an empty backbone (Nano-bit). RLU means Relative Luminescence Units. Data is represented as mean ± SEM; n = 3. P-values were obtained from Dunnett's Multiple Comparison Test; (***) P < 0.0001. ns means non-significant. 39

Figure 20 - The association between TRIB2 and AKT can be disrupted by TRIB3. We transiently transfected 293T cells with the indicated constructs for 24 hours. At the end point we added the luciferase substrate for 5 minutes and acquired the luminescence signal. As negative control we used non-transfected cells (Untransfected) and cells transfected with an empty backbone (Nano-bit). RLU means Relative Luminescence Units. Data is represented as mean ± SEM; n = 3. P-values were obtained from Dunnett's Multiple Comparison Test; (***) P < 0.0001. ns means non-significant.. 41

Figure 21 - The association between TRIB3 and AKT is stabilized by TRIB2. For this experiment we used 293T cell line. We did a 24h transiently transfection and acquired the luminesce 24 hours later, after 5 minutes exposure do luciferase substrate. As control we transfected only TRIB3 and AKT (absence of TRIB2), represented in the green bar. RLU means Relative Luminescence Units. Data are represented as mean ± SEM; n = 3. P-values were obtained from Dunnett's Multiple Comparison Test; (***) P < 0.0001. ns means non-significant. 42

Figure 22 – Analysis of AKT activation. For this experiment we performed a 24h transient transfection in 293T cells of increasing amounts of TRIB2 (panel A) and increasing amounts of TRIB3 (panel B). As controls, we used the 293T parental cell line (represented as 293T) and 293T transfected with an empty backbone (represented as Empty). Cells were lysed and proteins were extracted. 40 µg of total protein was loaded per lane and separated by 10% SDS-PAGE. The protein levels were assessed by western blot using specific antibodies against TRIB2 and TRIB3 (represented on the first band on the left and right, respectively), p-AKT Thr308, p-AKT Ser473, total AKT (t-AKT) and GAPDH. GAPDH was used as a loading control. ....

Figure 23 - 293T stable cell line expressing TRIB2. For this experiment we used 293T cell line. The stable transfection of TRIB2 enables the expression of TRIB2 on 293T cells that normally have none or low expression of this protein. As transfection controls we used the 293T parental cell line (represented as Parental) and cells transfected with an empty backbone (represented as

EMPTY); 40 µg total protein loaded per lane and separated by 10% SDS-PAGE. Protein levels were assessed with the specific tribbles antibodies by western blot technique. GAPDH was used as a loading control. MW means molecular weight. ....

Figure 24 - Co-immunoprecipitation of FLAG to detect the association of TRIB2 to AKT in the presence of increasing amounts of TRIB3. Experiment done in 293T lysates from cells stable transfected with TRIB2. Cells transiently transfected with increasing amounts of TRIB3 (MycHist-tagged), 500 ng of AKT (HA-tagged) and the remaining amount until 1500 ng transfected with an empty backbone *(pcDNA)*. The first three blots correspond to immunoprecipitated cell lysates with FLAG M2 beads (IP M2) and the last four blots correspond to the whole extract (WE) of cell lysates 40µg total protein loaded per lane and separated by 10% SDS-PAGE. Protein levels were assessed with the specific antibodies by western blot technique. GAPDH was used as a loading control. MW means molecular weight.. 46

Figure 25 - TRIB2 KO UACC-62 cell line. The fourth lane shows UACC-62 parental cell line. The other lanes correspond to different clones for TRIB2 KO, using two different guide RNAs targeting two different sequences of aminoacids of TRIB2 protein. All the clones were positive KO for TRIB2. 40 µg total protein loaded per lane and separated by 10% SDS-PAGE. Protein levels were assessed with the specific antibodies by western blot technique. GAPDH was used as a loading control. MW means molecular weight. ....

Tables Index

Table 1: List of the information about the antibodies used in this project.......... 29

Table 2 - Amount of DNA transfected into 293T to analyse TRIB2 and AKT interaction in the presence of TRIB3. Cells were transfected with 50 ng of TRIB2 and 50 ng of AKT. The amount of TRIB3 varied from 0 to 50 ng. The empty backbone (Nano-bit) was transfected as the remaining amount to a total of 150 ng. 40

Table 3 - Amount of DNA transfected into 293T cells to analyse TRIB3 and AKT interaction in the presence of TRIB2. 293T were transfected with 50 ng of TRIB3 and 50 ng of AKT. The amount of TRIB2 varied from 0 to 50 ng. The empty backbone (Nano-bit) was transfected as the remaining amount to a total of 150 ng. 42

Abbreviations

ABC	ATP Binding Cassette
AJCC	American Joint Committee on Cancer
AML	Acute Myelogenous Leukemia
ATP	Adenosine Triphosphate
BCL-2	B-Cell Lymphoma 2
CO2	Carbon Dioxide
CTL	Cytotoxic T-lymphocytes
CTL-4	Cytotoxic Lymphocite associated antigen 4
CYP	Cytochrome P450
DDR	DNA damage response
DMEM	Dulbecco’s Modified Eagle’s Medium
DTIC	Dacarbazine
EMT	Epithelial to MesenchymalTransition
FBS	Fetal Bovine Serum
FDA	Food and Drug Administration
FOXO	Forkead BoxO
GPCR	G protein coupled receptor
HR	Homologous recombination
IL-2	Interleukin-2
MDM2	Mouse double minute 2
MMR	Mismatch Repair
NER	Nucleotide Excision Repair
OS	Overall Survival
PD-1	Programmed Cell Death Protein 1
PDK1	Phosphoinositide-dependent kinase-1
PFS	Progression Free Survival
PH	Pleckstrin homology
PI3K	Phosphatidylinositol 3-kinase
PIP2	Phophoinositide-(3, 4)-P2
PIP3	Phophoinositide-(3, 4, 5)-P3

RTK	Receptor Tyrosine Kinase
Ser473	Serine 473
SNL	Sentinel Lymph Nodes
TMZ	Temozolomide
TRIB	Tribbles
TRIB2	Tribbles homolog2
TRIB3	Tribbles 3
UV	Ultraviolet
VLS	Vascular Leak Syndrome
WHO	World Health Organization
PBS	Phosphate Buffered Saline
HEK	Human Embryonic Kidney
Rpm	Revolutions per minute
PIC	Protease Inhibitors Cocktail
BSA	Bovine Serum Albumine
SDS-Page	Sodium dodecyl sulfate polyacrylamide gel eletrophoresis
APS	Ammonium Persulfate
TEMED	Tetramethylethylenediamine
ECL	Enhanced Chemiluminescence
HRP	Horseradish peroxide
PCA	Protein Complementarion Assay
sgRNA	Small guide RNA
PAM	Protospacer Adjacent Motif
NHEJ	Non Homologous End Joining

Introduction

1 Introduction

1.1 Cancer

Cancer is a leading cause of death worldwide. A study revealed that there were 14.1 million new cases and 8.2 million deaths in 2012 [6]. Unfortunately, these numbers tend to increase. Cancer is set to become the major cause of morbidity and mortality in the coming decades. By 2030, 20.3 million new cancer cases and more than 13 million cancer deaths are expected [7].

At the cellular level, cancer is viewed as a multistep process involving mutations and selection of cells with increasing proliferation, survival, invasion and metastatic capacity [8]. These mutations can affect oncogenes or tumor-supressor genes operating similarly at the physiologic level: by increasing tumor cell number through the stimulation of proliferation or the inhibition of cell death. A third class of genes, known as stability genes or caretakers, include the mismatch repair (MMR), nucleotide-excision repair (NER) and base-excision repair (BER) genes and are responsible for repairing mistakes made during the replication of DNA or induced by exposure to mutagens [9]. When stability genes are inactivated, mutations occur at a higher rate [10].

In 2000 Hanahan and Weinberg suggested “a small number of molecular, biochemical, and cellular traits - acquired capabilities - shared by most and perhaps all types of human cancer”, widely known as the Hallmarks of Cancer. The first six hallmarks described included: self-sufficiency in growth signals, insensitivity to anti-growth signals, evading apoptosis, sustained angiogenesis, limitless replicative potential and tissue invasion and metastasis [11]. Eleven years later, in 2011 the same authors updated this list including two more hallmarks essential for malignant transformation: genomic instability and inflammation. In addition, there are two more capabilities emerging: the metabolic reprogramming and avoidance of the immune system, as shown in Figure 1 [4].

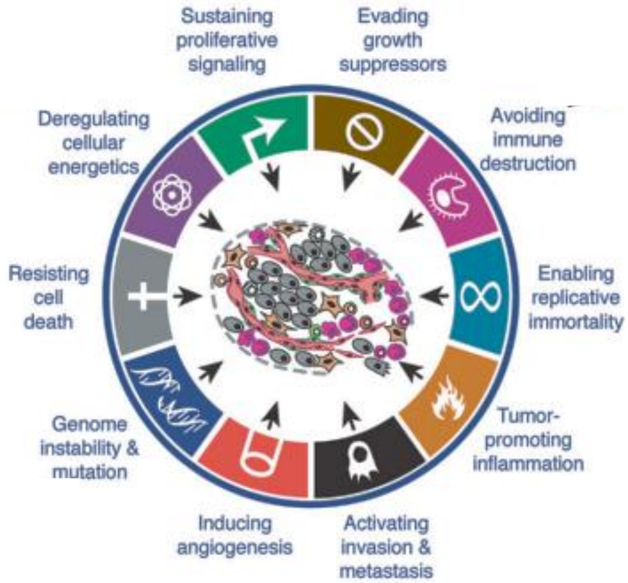
Sustaining proliferative signaling
Evading growth suppressors
Avoiding immune destruction
Enabling replicative immortality
Tumor-promoting inflammation
Activating invasion & metastasis
Inducing angiogenesis
Genome instability & mutation
Resisting cell death
Deregulating cellular energetics

Figure 1 - The hallmarks of cancer. A normal cell needs to overcome several mechanisms to become transformed. The first described hallmarks were: self-sufficiency in growth signals, insensitivity to anti-growth signals, evading apoptosis, sustained angiogenesis, limitless replicative potential and tissue invasion and metastasis. In 2011 the same authors suggested two more hallmarks involved in tumorigenesis: genomic instability and tumor promoting inflammation. New capabilities have been emerging in the last years: the ability of cancer cells to reprogram its metabolism and to avoid the immune system mediated destruction. Adapted from Hanahan D. and Weinberg R., “The Hallmarks of cancer”, Cell, 2011 [4]

1.2 Melanoma

Melanoma is the most aggressive skin cancer with constantly rising incidence worldwide, especially in fair-skinned populations, as represented in Figure 3.

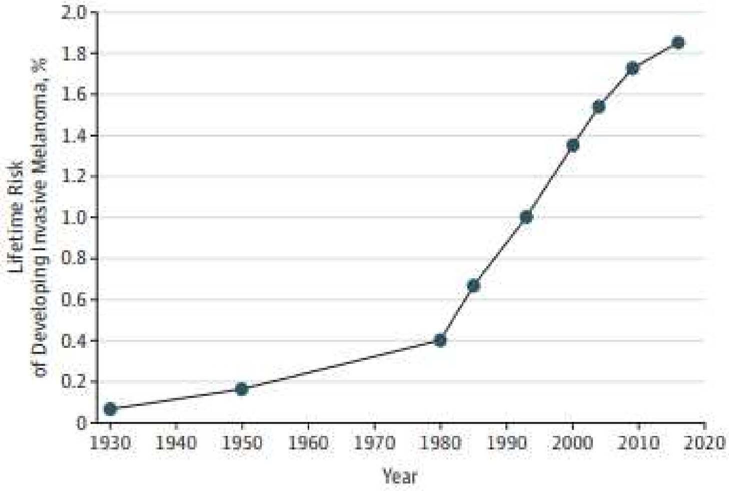

Figure 3: **Changes in annual lifetime risk of developing invasive melanoma in the United States from 1930 to 2016.** Adapted from "Analysis of trends in US melanoma incidence and mortality", JAMA Dermatology, 2017 [3].

Despite accounting for only 5% of all skin cancers, malignant melanoma is responsible for 80% of skin cancer deaths [12]. The World Health Organization (WHO) estimates that each year 132 000 new cases of melanoma are diagnosed, and this type of cancer has a mortality rate that continues to rise through the last years, as represented in Figure 2.

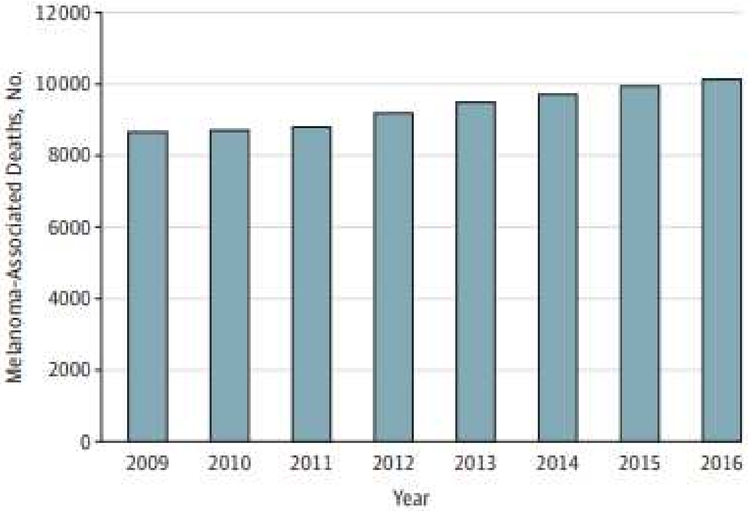

Figure 2: **Estimated number of annual deaths from melanoma in the United States from 2009 to 2016**. Adapted from "Analysis of trends in US melanoma incidence and mortality", JAMA Dermatology, 2017 [3].

Melanoma arises from the transformation of the melanocytes - the pigment-producing cells of the human skin that are localized within the basal layer of the epidermis. These cells are mainly found in the skin and hair follicles, but they also can be found in the ocular pigment epithelium. The main function of melanocytes is the synthesis, storage, and transfer of melanin pigments to the surrounding epithelial cells - resulting in the tanning response [13, 14].

Melanocytes are derived from the neural crest so, soon in embryonic development, these cells undergo epithelial to mesenchymal transition (EMT) to exit the neural tube and migrate to the skin of the whole body. In a similar way, malignant melanoma cells access the circulatory or lymphatic system and migrate to a new location, establishing metastases. Due to the fact that these cells just need to “remember how to migrate”, melanoma is known to be one of the most metastatic cancers and the 5-year survival rate of patients with metastatic melanoma is less than 5% [15, 16].

Apart from the family history, fair skin and immunosuppression, the major risk associated with melanoma progression is the ultraviolet (UV) radiation exposure. Solar radiation, UVA and UVB, can mutagenize DNA, often producing UV landmark mutations: C to T or CC to TT substitutions. When these mutations affect critical oncogenes and tumor-suppressor genes, transformation of melanocytes occur as shown in Figure 4 [17].

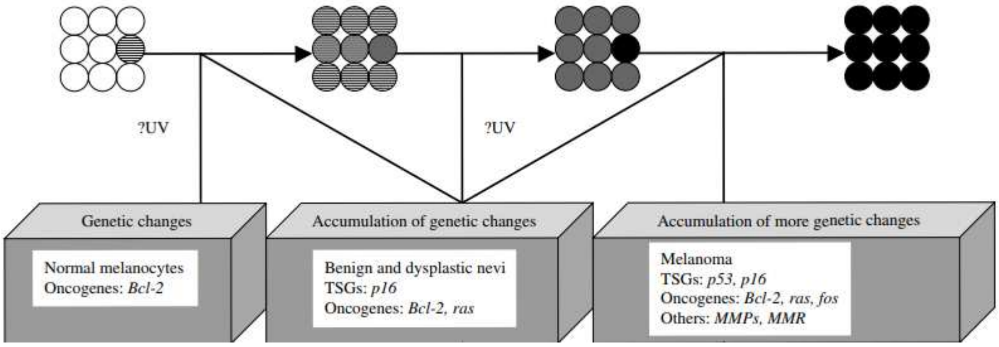
?UV
?UV
Genetic changes
Normal melanocytes
Oncogenes: *Bcl-2*
Accumulation of genetic changes
Benign and dysplastic nevi
TSGs: *p16*
Oncogenes: *Bcl-2*, *ras*
Accumulation of more genetic changes
Melanoma
TSGs: *p53*, *p16*
Oncogenes: *Bcl-2*, *ras*, *fos*
Others: *MMPs*, *MMR*

Figure 4 - Cutaneous transformation of melanocytes. The accumulation of genetic changes induced by UV light both in tumor suppressor genes and oncogenes are responsible for the transformation of the pigment producing cells of the human skin. Adapted from Hussein, Mahmoud R., “Ultraviolet radiation and skin cancer: molecular mechanisms”, Journal of Cutaneous Pathology, 2005 [17].

1.2.1 Clinical Grading System

Staging of cancer is fundamental to provide physicians and patients with prognostic information and to guide therapeutic decisions [5]. Melanoma progression's international staging system was developed by the American Joint Committee on Cancer (AJCC) and it categorizes melanoma into five different stages according to tumor thickness, number of metastatic nods and distant metastasis, as represented in Figure 5.

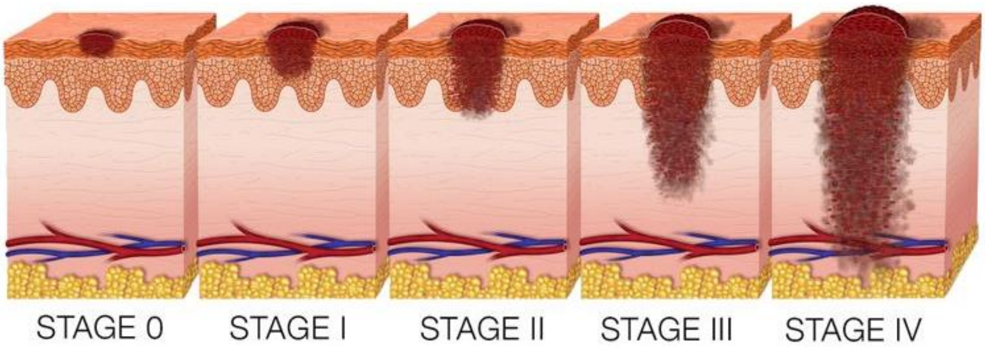

Figure 5 - Stages of melanoma. The first stage is the less aggressive, cell proliferation is limited to the epidermis, not reaching the dermis so the treatment applied in this case in only the surgical resection. Melanomas on stages I and II are characterized by tumor thickness and ulceration and are treated by surgical resection followed by drug or radiation treatment. When cancer cells are already spread to the lymph nodes is stage III and surgical removal of the lymph nodes is required. If cancer has spread into distant organs it is a IV stage melanoma and is treated with chemotherapy [5].

1.2.2 Melanoma genetics

The high prevalence of BRAF (50%) and NRAS (20%) mutations strongly correlate the RAS-RAF-MEK-ERK signalling, also known as MAPK pathway, with the aggressive biology of melanoma. However, both activating BRAF and NRAS mutations are found in tumors with very little malignant potential as benign nevi [18]. Furthermore, it has been shown that the expression of BRAF alone fails to transform benign melanocytes [19]. Finally, some tumors with resistance to BRAF inhibitors continue to survive and proliferate despite continued inhibition of the RAS-RAF-MEK-ERK signalling pathway [20]. Thus, the activation of the RAS-

RAF-MEK-ERK alone is not sufficient to fully explain the pathogenesis of this aggressive cancer [21].

1.2.3 PI3K-AKT pathway

Activation of the phosphatidylinositol 3-kinase (PI3K)-AKT pathway is one of the most frequent events in cancer [22]. This pathway plays a significant role in melanoma, frequently in the setting of concurrent activation of MAP kinase pathway [21-24]. Furthermore, the activation of the PI3K-AKT pathway is correlated with poor clinical outcomes and resistance to MAPK pathway inhibitors used for melanoma treatment [25].

The PI3K-AKT pathway can be activated by different factors including binding of ligands by receptor tyrosine kinases (RTKs), G protein-coupled receptors (GPCRs) and GTP binding of RAS proteins. Any of these signals can activate the catalytic activity of PI3K. Then PI3K phosphorylates the 3rd position of the inositol ring of lipids in the plasma membrane, resulting in the conversion of phosphatidylinositol-(3,4)-P2 (PIP2) to phosphatidylinositol-(3,4,5)-P3 (PIP3). PIP3 interacts with pleckstrin homology (PH) domains of intracellular proteins, resulting in its recruitment to the inner surface of the cellular membrane. One such protein is AKT, as shown on Figure 6 [21].

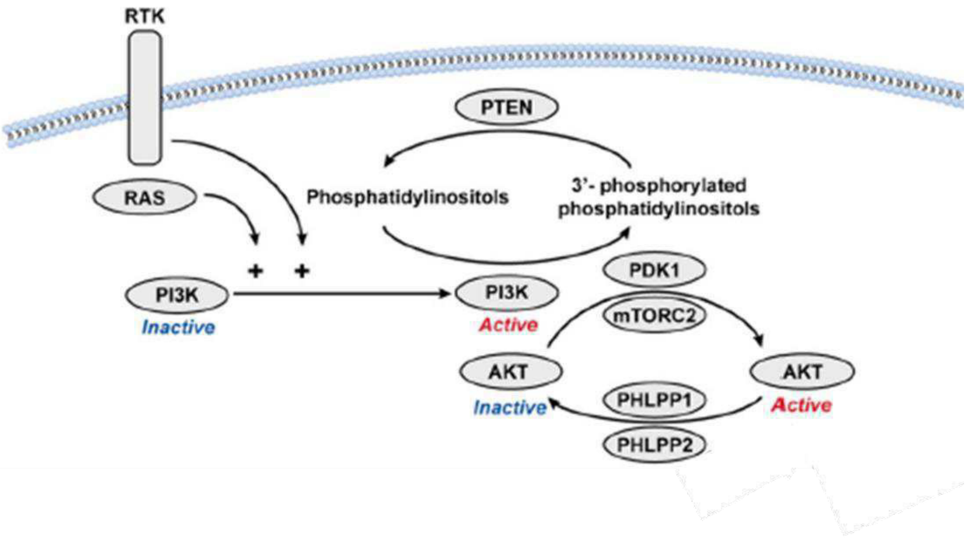

Figure 6 - The PI3K-AKT pathway. Diagram of key activators and regulators of the PI3K-AKT signalling network. Adapted from Davies, Michael A., "The role of the PI3K-AKT Pathway in Melanoma", The Cancer Journal, 2012 [21].

AKT has 3 highly homologous isoforms: AKT1, AKT2 and AKT3. It is a serine-threonine kinase that normally exists in the cytoplasm in an inactive form. Upon activation of PI3K, AKT is recruited to the plasma membrane (by its PH domain) and then it can be phosphorylated at 2 critical residues: Thr308 and Ser473. The Thr308 is phosphorylated by phosphoinositide-dependent kinase1 (PDK1), which also has a PH domain being recruited to the plasma membrane. Ser473 of AKT is phosphorylated by the mTORC2 complex in response to growth factor stimuli. AKT is activated in more than 60% of melanoma patients [26]. AKT can be inactivated by the phosphatases PP2A and PHLPP1/2. PTEN dephosphorylates the 3rd position of PIP3 directly antagonizing the activity of PI3K, as represented in Figure 6. In this sense, loss of PTEN, that occurs in up to 30% of melanoma patients, results in constitutive activation of the PI3K-AKT pathway [21, 27].

1.2.4 Melanoma treatment options

Melanoma resection

The first treatment choice for patients with early- and intermediate-stage of disease (stage I and stage II) is surgical resection. It consists on the resection of the entire melanoma and surrounding skin, including the epidermis, dermis and subcutaneous fat.

The presence of cancer cells in regional lymph nodes is the most important prognostic indicator for melanoma patients [28]. Since the lymphatic system is the first rout of metastasis in melanoma, it provides information about the disease progression. Therefore, the identification and evaluation of the first node or nodes draining the primary melanoma along its lymphatic pathway which are called sentinel lymph nodes (SLN), is crucial for staging, prognostication and making treatment decisions [29]. If the presence of melanoma cells is confirmed in the lymphatic system the standard medical procedure is perform a complete lymphadenectomy to remove all the metastatic cells present in the lymphatic pathway [30].

Chemotherapy

Chemotherapy has a more prominent role in melanomas which do not harbour somatic mutations that can be targeted with specific inhibitors. This type of therapy relies on inhibiting the division of rapidly growing cells, such as cancer cells. However, rapid division rate also occurs in normal bone marrow cells, skin cells, gastrointestinal cells and hair follicle cells. Therefore, the fact that chemotherapeutic agents do not target specifically cancer cells is the major cause of associated toxicity and side effects of general chemotherapy [31].

The first chemotherapeutic agent used to treat patients with advanced melanoma was dacarbazine (DTIC) which is an alkylating agent. Treatment with DTIC results in DNA adducts, preventing the multiplication of rapidly growing cells. DTIC has an overall response rate between 10%-20% and allows a complete remission in only 5% of melanoma patients [32]. DTIC is an intravenous infusion and the main side effects include nausea, vomiting and myelosuppression.

Another chemotherapeutic agent that is used in the treatment of advanced-stage melanoma is temozolomide (TMZ). Similar to DTIC, TMZ is an alkylating agent. It is an oral chemotherapeutic drug and due to its small weight, it can cross the blood-brain barrier, and is widely used to treat patients with melanoma metastasis in the brain [33]. The main side effects include headache, nausea, vomiting, lymphopenia and thrombocytopenia [34].

A randomized phase III trial of DTIC versus TMZ in patients with metastatic melanoma demonstrated similar survival response rates - 12.1% for DTIC-treated patients and 13.5% for temozolomide-treated patients.

Other cytotoxic chemotherapeutic drugs have been tested for the treatment of advanced melanoma such as nitrosaureas (Carmustine), vinka alcaloids (Vincristine), taxanos (Taxol) and platinium compounds (Cislatin) but have shown no benefits compared to DTIC or TMZ [35, 36].

Immunotherapy

Chemotherapy regimens can be beneficial for some patients with advanced melanoma, but none have led to a significant improvement in overall survival. For this reason, additional treatment options have become available in the last years.

Melanoma is a particularly immunogenic tumor what makes this type of cancer a good candidate for immunotherapy [37]. The ability of melanoma cells to induce an immune response is associated with the high mutation load of this type of cancer, as shown in Figure 7. As mutational load depends on the exposure to carcinogens, tissues directly exposed to carcinogenic substances, such as skin and lung, tend to have a high mutational load. Melanoma has a high prevalence of somatic mutations leading to the presentation of several neoantigens on the cell surface of cancer cells. These neoantigens are seen as “strange epitopes” and trigger an immune response.

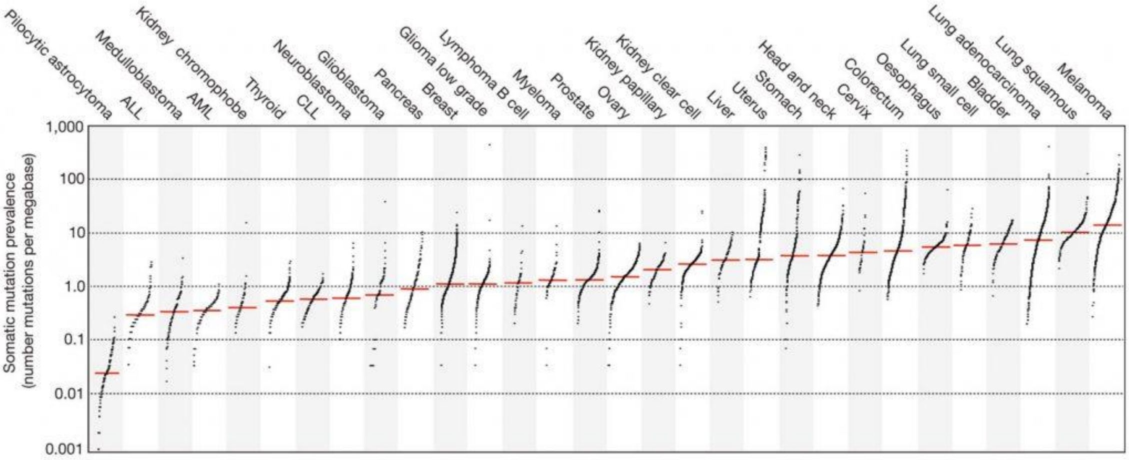

Figure 7 - Signatures of mutational processes in human cancer. Cancer with high mutational load respond better to immunotherapy and tend to be highly resistant to traditional treatments. Adapted from “Signatures of mutational process in human cancer”, Nature, August 2013 [38].

Immunotherapy using checkpoint inhibitors is defined as the use of the patient immune system to treat cancer and it involves the inhibition of regulatory cell surface molecules which act normally to dampen or modulate T-cell activation.

Interleukin-2 (IL-2) was one of the first immunotherapeutic drugs used since the 1990´s but it is still not clear how IL-2 works as an anti-cancer therapy. It is thought that the exogenous IL-2 may promote a Cytotoxic T lymphocytes (CTL)-mediated anti-tumor response [39]. IL-2 has shown some toxicity associated with vascular leak syndrome (VLS), which leads to interstitial edema and general organ failure [40]. Over the last years three new immunotherapeutic drugs have been approved by Food and Drug Administration (FDA) and many more are in clinical trials for the treatment of melanoma. The first of these drugs to be approved was Ipilimumab, an antagonist to CTLA-4 (Cytotoxic lymphocyte-associated antigen 4). More recently antagonists of Programmed Cell Death

Protein 1 (PD-1) Nivolumab and Pembrolizumab followed. Both Nivolumab and Pembrolizumab negatively regulate the immune system, maintaining self-tolerance and avoiding auto-immune response [41]. Cancer cells often take advantage of this regulatory immune mechanism, blocking immune responses against them. Anti-CTLA-4 antibodies bind to the CTLA-4 receptor, blocking its downstream signalling pathway thereby allowing T-cell activation and proliferation. Therefore, in the presence of this drug the immune system is capable of destroying melanoma cells in a subset of patients[42]. Similarly, PD-1 is also an immune checkpoint protein found on the surface of cells. Upon binding to its two ligands PD-L1 and PD-L2, PD-1 negatively regulates the activity of T-cells at a variety of stages of the immune response. When engaged by the ligands, PD-1 inhibits kinase signalling pathways that normally lead to T-cell activation [43]. [44, 45]. However, not all patients with melanoma respond to this treatment and it can have considerable side effects. Moreover, it is not possible to predict which patients are likely to respond to therapy and which patients are not. [46]

Targeted therapies

Targeted therapies interfere with a specific molecular target that drives cancer cell growth and survival. For melanoma treatment much attention has been focused on developing inhibitors of the most hyperactivated pathways in this type of cancer: MAPK and PI3K pathways. BRAF is a serine-threonine protein kinase belonging to the RAF family of kinases, which is part of the MAPK signalling pathway, represented in Figure 8. Under normal, non-cancerous conditions, binding of a growth factor to a RTK activates RAS, which in turn activates the RAF kinases: A-RAF, B-RAF and C-RAF. Activated RAF in turn phosphorylates and activates MEK, another kinase leading to its activation and the phosphorylation of the downstream kinase ERK and subsequent activation of several targets that result in cell proliferation and survival. The dysregulation of the MAPK pathway is a key event in the development of melanoma. Activating BRAF mutations are present in about 50% of all melanomas, most commonly, resulting in a substitution of a glutamic acid for a valine at position 600 (V600E) [47]. This mutation leads to a constitutive active MEK and thus, hyperactivated ERK.

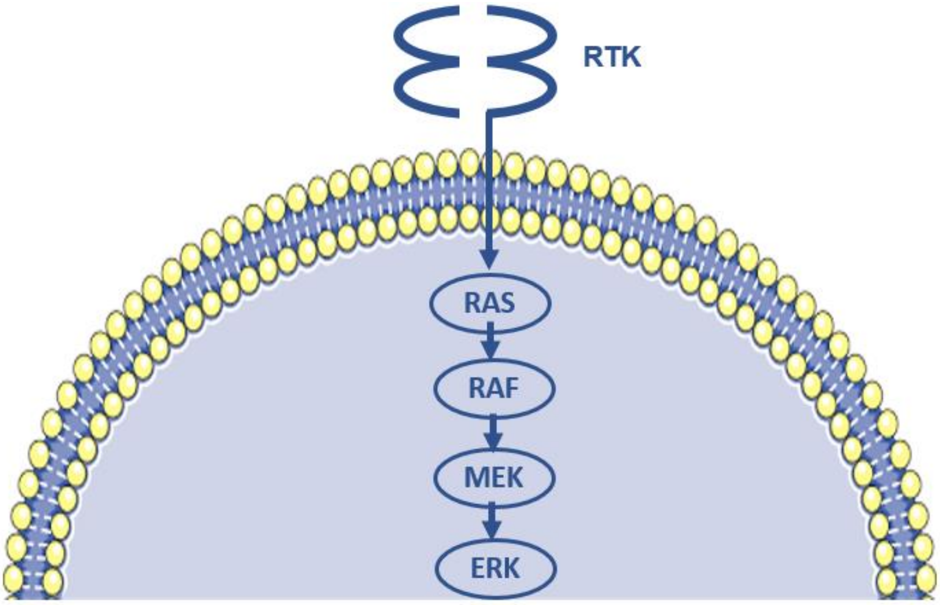

Figure 8 - Overview of the MAPK pathway. Activation of a cell surface receptor tyrosine kinase (RTK) leads to a sequential phosphorylation and activation of proteins in the MAPK pathway: RAS, RAF, MEK and ERK. ERK activation mediates phosphorylation of key proteins involved in cellular proliferation and survival. Adapted from [2].

The clinical outcome for patients with advanced melanoma carrying B-RAF mutations, significantly improved with the use of specific BRAF and MEK inhibitors. Two clinically relevant BRAF inhibitors are vemurafenib (Zelboraf) and dabrefinib (Tafinlar). Treatment of advanced melanoma patients harbouring the BRAF^{V600E} mutation with vemurafenib, the first BRAF inhibitor approved by the FDA in 2011, resulted in tumor regression in over 80% of patients, having a positive impact on progression-free survival (PFS) and overall survival (OS) [48, 49]. The mechanism of action of vemurafenib involves the selective inhibition of the mutated BRAF^{V600E} kinase, reducing the MAPK signalling activity. The adverse effects associated with almost every patient treated with vemurafenib, include rash, fatigue, arthralgia, alopecia, photosensitivity and nausea. Despite the initial positive response to treatment with vemurafenib or dabrefenib, the durability of response is limited by the development of drug resistance by the patients in the next 6 to 8 months [50, 51]. There are several mechanisms by which cancer cells can reactivate the MAPK pathway but, in most cases, it is due to activating mutations on downstream targets of BRAF such as MEK and ERK [52]. Considering this, an alternative strategy would be to develop inhibitors of downstream effectors of BRAF, such as MEK inhibitors.

The FDA approved the first MEK inhibitor, Trametinib, in 2013. Trametinib (Mekinist) is an orally available, small-molecule, selective inhibitor of MEK1/2 [53-55]. In a phase 3 clinical trial, 322 patients with metastatic melanoma and BRAF mutations were randomized to receive either trametinib or chemotherapy (DTIC or paclitaxel). The OS rate at 6 months was 81% in the trametinib group and 67% in the chemotherapy group [56].

Targeting the MAPK and PI3K/AKT signaling pathways in melanoma with selective inhibitors has produced remarkable antitumor activity. However, the development of resistance to these therapies remains a major barrier to complete tumor eradication [57].

1.2.5 Resistance mechanisms

Drug resistance is a phenomenon that results when disease become tolerant to pharmaceutical treatments. The mechanisms underlying resistance are represented in Figure 9 and include drug inactivation, drug efflux or the ability of cancer cells to increase the DNA damage repair [58]. Resistance mechanisms can be intrinsic or acquired. Intrinsic resistance means that it already existed before the treatment. Conversely, acquired resistance occurs after the treatment meaning that the tumor was initially sensitive to the therapy.

Melanoma is one of the most therapy-resistant types of cancer. Despite the encouraging results of immune checkpoints inhibitors, the majority of patients are either intrinsically resistant or rapidly develop resistance to this therapy [59]. Similarly, melanoma patients treated with MAPK pathway inhibitors, develop resistance in less than a year [60]. Half of the patients treated with vemurafenib or dabrafenib monotherapy develop drug resistance within 6-8 months of treatment [61].

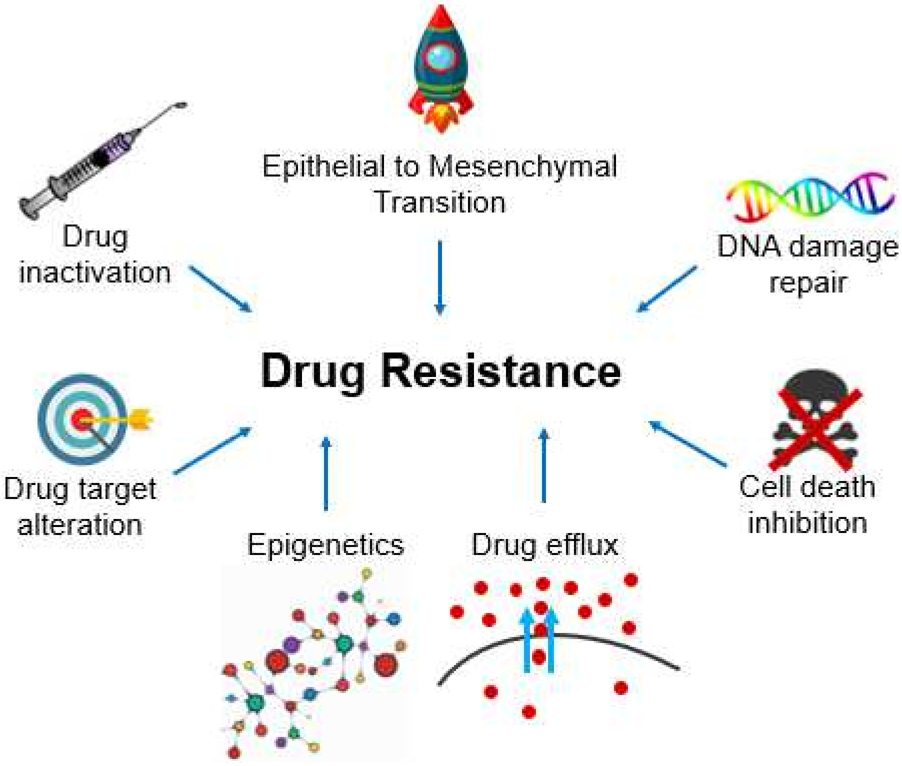
Epithelial to Mesenchymal Transition
Drug inactivation
DNA damage repair
Drug Resistance
Drug target alteration
Cell death inhibition
Epigenetics
Drug efflux

Figure 9 - Resistance mechanisms to cancer therapy. The main mechanisms that can enable or promote direct or indirect drug resistance in human cancer cells include drug inactivation, drug efflux or the ability of cancer cells to increase the DNA damage repair. Adapted from [58].

Drug inactivation

Many anticancer drugs must undergo metabolic activation before having clinic efficacy. However, some cancer cells can downregulate the enzymes responsible for drug activation. [62]. Important examples of drug activation and inactivation enzymes include the cytochrome P450 (CYP) system, a superfamily that activated or deactivates the drug [63, 64]. Mutations or alterations in constituents of the CYP system may change the proteins' metabolic capabilities such as increasing the breakdown of drugs and their secretion by kidneys. Therefore, the drug intracellular levels would not be maintained and the cancer would be considered resistant to it [65].

Drug Efflux

Reducing drug concentration by enhancing drug efflux is one of the most studied mechanisms of cancer drug resistance [66]. ATP-binding cassette (ABC) transporters are a superfamily of proteins responsible for the transport of a broad variety of drugs outside the cell. This mechanism plays an important role in preventing accumulation of toxins within the cell but, in cancer conditions these proteins were found to be overexpressed removing the drug from the cell [67].

DNA damage repair

In response to chemotherapy drugs that directly or indirectly damage DNA, DNA damage response (DDR) mechanisms can reverse drug-induced damage, inhibiting the apoptotic processes and cancer cell death [68]. Cisplatin, a platinium-containing chemotherapy drug, cause harmful DNA crosslinks in cancer cells, which can lead to apoptosis. Nucleotide excision repair (NER) and homologous recombination (HR) are the primary DNA repair mechanisms involved in reversing this damage, contributing to drug resistance in these cases [69].

Cell death inhibition

Apoptosis has two established pathways: an intrinsic pathway mediated by the mitochondria that involves B-cell lymphoma 2 (BCL-2) family proteins and caspase-9, and an extrinsic pathway that involves death receptors on the cell surface. Both pathways merge through the activation of downstream caspase-3 which ends up causing apoptosis [58]. In several types of cancers, such as melanoma, BCL-2 proteins, AKT and other anti-apoptotic proteins are more activated having a negative effect on apoptosis, allowing the survival of cancer cells and contributing to drug resistance [70].

Epithelial-Mesenchymal Transition and Metastasis

The epithelial to mesenchymal transition (EMT) is a mechanism by which solid tumors become metastatic. It is a complex mechanism that can involve the formation of new blood vessels (angiogenesis), the reduction of the expression of cell adhesion receptors (integrins and cadherins, and the increase expression of cell adhesion receptors to induce cell motility [71]. The EMT has been found to play a critical role in cancer drug resistance but the nature of this link remains unclear [71].

1.2.6 Tribbles

The Link laboratory has discovered a novel mechanism of drug resistance, facilitated by the oncoprotein Tribbles homolog 2 (TRIB2), to a broad spectrum of drugs used in clinical trials (BEZ235, a PI3K/mTORC inhibitor, BAY236 and

BAY1082439, both PI3K inhibitors, rapamycin, a mTORC inhibitor) or which are already in use for melanoma treatment (DTIC, gemcitabine and 5-fluoruracil).

The Tribbles (TRIB) pseudokinases proteins were first described in 2000 as major regulator of *Drosophila* morphogenesis by inhibiting mitosis. Tribbles were identified in a genetic screen that aimed to identify mutations that control cell division and cell migration during embryonic *Drosophila* development [72, 73].

Tribbles encodes an evolutionary conserved family of proteins characterized by the presence of a N-terminal domain, a central serine-threonine kinase like domain, a C-terminal domain that contains a COP-1 binding domain for E3 ubiquitin ligases and a MEK-1 binding domain which mediates the interaction with multiple MAPKKs proteins, as represented on Figure 10. Tribbles are considered catalytically inactive because they lack some conserved residues on the ATP (Adenosine Triphosphate) binding site. However, recent data suggested that TRIB2 has the ability to hydrolyse ATP *in vitro*, showing a weak kinase activity [74].

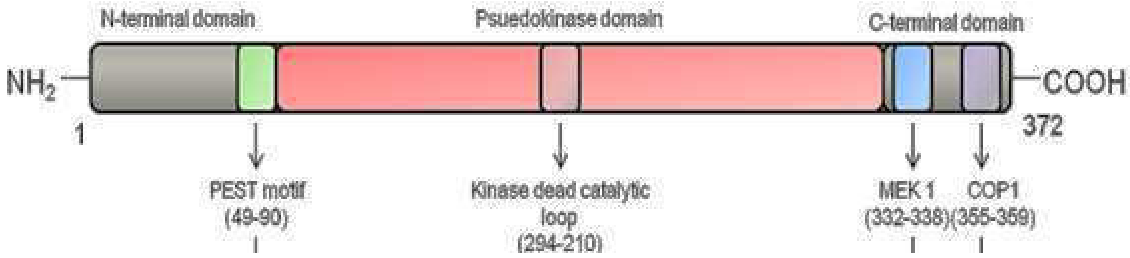

Figure 10 - Structure of Tribbles family. Tribbles structure has three main domains: a central serine-threonine kinase like domain (resembles a kinase domain but has some aminoacids lacking that are essential to the catalytic activity), a MEK-1 and a COP-1 binding domain. Adapted from [1].

In mammals three genes of TRIB homologues have been described: TRIB1, TRIB2 and TRIB3. Tribbles family members are expressed in different tissues, as shown on Figure 11, and control multiple aspects of eukaryotic cell biology that include glucose and lipid metabolism, inflammation, cellular stress, survival, apoptosis and tumorigenesis [75].

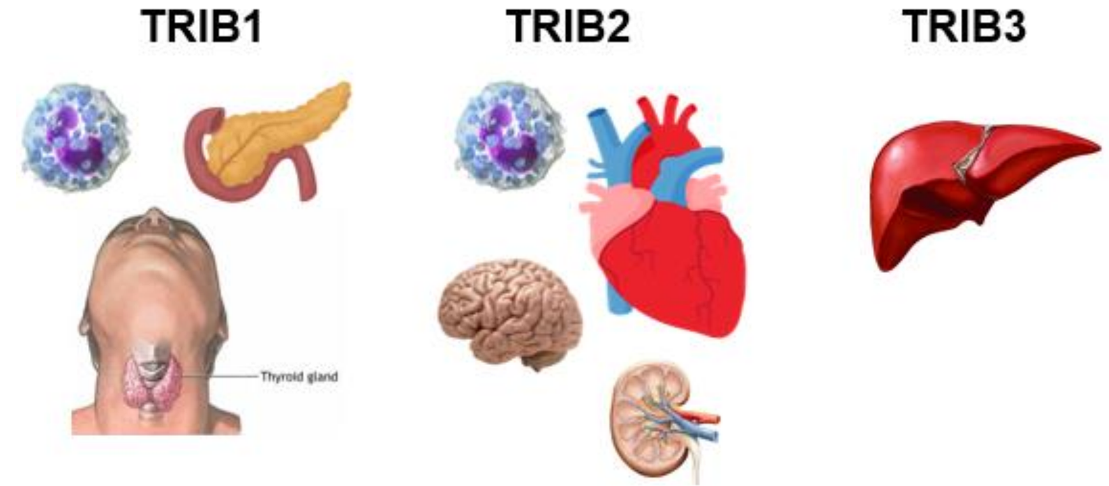

Figure 11 - Tribbles tissue expression. TRIB1 is highly expressed in the bone marrow, peripheral blood leukocytes, thyroid gland and pancreas [76, 77]. TRIB2 is highly expressed in peripheral blood leukocytes, thymus, heart, brain, kidney, lung, skin and white adipose tissue [76, 77]. TRIB3 is more expressed in human liver [76].

The mechanism of action of these proteins is not fully understood but it is thought that Tribbles function as scaffold proteins contributing to stabilize and support the modulation of signaling pathways as MAPK pathway. The atypical pseudokinase domain also retains a regulated binding platform for substrates which are then ubiquitinated by specific E3 ligases, facilitating the ubiquitin-mediated degradation of some proteins [1, 78].

Recently, the study of the formation of protein complexes involving tribbles that then dictate cellular signaling is an emerging theme in tribbles biology [1]. TRIB1 and TRIB2 appear to function as oncogenes in acute myelogeneous leukemia (AML) [77]. Furthermore, the Link laboratory also correlated high levels of TRIB2 with melanoma disease staging and clinical progression, suggesting TRIB2 as a biomarker for diagnosis and progression of melanoma patients [12]. TRIB3 has been proposed to act as an inhibitor of AKT, having a tumor suppressor activity [79].

The role of TRIB2 in melanoma prognosis

TRIB2 was discovered to be a repressor of the tumor suppressor Forkhead BoxO (FOXO), through a screening for FOXO repressor proteins [80]. High levels of TRIB2 were shown to facilitate the growth and survival of melanomas by deregulating FOXO activity [12]. As FOXO proteins play an important role in supressing cell survival and proliferation through regulation of the expression of apoptotic proteins and cell cycle regulators, proteins that are capable of supressing FOXO activity are strong candidates to have a direct role in cancer initiation, maintenance, progression and to confer drug resistance [81].

Furthermore, the high TRIB2 protein levels found in melanoma patients were correlated with high AKT activation, more precisely - with high levels of phosphorylation of the serine 473 (Ser473) of AKT [82]. It has been demonstrated that the association between TRIB2, via the COP-1 domain, and AKT causes an increased phosphorylation of the serine 473 of AKT via mTORC2, activating AKT and culminating in high levels of cell proliferation and survival. Through these studies they demonstrated that cell lines with higher TRIB2 protein levels correlated with AKT activation through its phosphorylation on serine 473 and with increased total AKT. In melanoma cells with TRIB2 depletion the levels of phosphorylation of Ser473 of AKT and total AKT were lower compared to melanoma cells where TRIB2 was not depleted [82]. Furthermore, TRIB2 overexpression increased the levels of AKT pSer473 and the levels of total AKT before and after the treatment with PI3K and mTOR inhibitors, suggesting that these drugs may not be clinically efficient in patients with high levels of TRIB2. Link et al suggested that TRIB2 and AKT interact, forming a protein complex and promoting AKT activation [82]. AKT activation leads to the phosphorylation of FOXO3a (a tumor suppressor gene) for proteasome degradation and also activates E3 ubiquitin ligase mouse double minute 2 homologue (MDM2) with consequent inhibition of apoptosis mediated by p53 [83]. MDM2 functions as a E3 ligase that ubiquitinates p53 for degradation blocking its transcriptional activity and culminating in uncontrolled cancer cell proliferation [82, 84].

The role of TRIB3 in cancer

Intriguingly, tribbles pseudokinase 3 (TRIB3) has been proposed to exert the opposite effect on AKT by other groups, including one of our collaborators from England, Dr. Endre Kiss-Tooth [85-87].

TRIB3 has been proposed to act as an inhibitor of AKT although the precise molecular basis of this activity and whether the loss of TRIB3 contributes to cancer initiation and progression remain to be clarified. TRIB3 has been suggested to interact with different targets including MAPKs and several transcription factors [85].

It has been shown that the genetic inhibition of TRIB3 facilitates oncogene transformation and enhances the tumorigenicity of cancer cells, suggesting that TRIB3 has an oncossupressive function. TRIB3 has also been shown to interact and inhibit AKT [86, 87]. In addition, the loss of TRIB3 enhances the phosphorylation of AKT in cancer cells via mTORC2, promoting FOXO inactivation [79]. Moreover, TRIB3 is found to be focally deleted in tumors of epithelial origin and in breast cancer patients. In addition, analysis of gene expression profiles of cancer patients from published studies reveals that TRIB3 mRNA levels are downregulated in different tumor types [79].

1.3 Hypothesis

TRIB2 and TRIB3 are proposed to play an opposing role in tumorigenesis by controlling the PI3K/AKT pathway so the balance between TRIB2 and TRIB3 expression may be a critical factor underlying melanoma pathogenesis and response to therapy. Taking this into account we hypothesize that TRIB2 and TRIB3 compete for AKT binding.

Methodology

2 Methodology

2.1 Cell culture

Cell culture is a tool by which the behaviour of the cells can be studied independent of the whole organism. In this method cells are grown under controlled, favourable and artificial conditions providing an important system to study a range of diseases.

All the procedures below were performed under sterile conditions using a Laminar Flow Chamber (Microflow, advanced biosafety cabinet class II, UK). The cell lines used in this study were maintained using Dulbecco's Modified Eagle's Medium (DMEM) with Ultraglutamine and 4.5 g/L Glucose (Lonza, Verviers, Belgium) supplemented with 10% Fetal Bovine Serum (FBS;Biowest, South America) and 1% Penicillin/Streptomycin (Amresco, Ohio). The cells were cultured in 10 cm plates (SLP Life Sciences, Korea) and maintained in an incubator (Thermo Electron Corporation 311, Canada) at 37 ºC and 5% carbon dioxide (CO_2). When cells reached 70-80% confluency they were detached from culture flasks and replated onto new culture flasks. Cells were washed with 1x Phosphate Buffered Saline (PBS; Sigma Aldrich, USA) and coated with 1.5x trypsin (Sigma Aldrich, USA) diluted in 1x PBS. Trypsin is a member of serine protease family and, by cleaving peptides, trypsin allows cells to detach from the culture plate.

2.1.1 Cell count

To plate a specific number of cells, they were counted using a Neubauer chamber (Blau brand, Germany). We used 10 µL of the cell suspension and mixed it with 10 µL of Trypan Blue (Sigma Aldrich, UK). Then we transferred 10 µL of the solution to the Neubauer chamber and we counted the number of cells present in the four external corners, represented on Figure 12.

Cell concentration was calculated according to the following equation $(X_1+X_2+X_3+X_4)/4 \times 2 \times 10^4$ cells/ml. It means that we divided the average number of cells present in every square for the dilution factor of our solution and then we divided the result by the volume of the chamber (it has 0.1mm of depth so the volume is 0.1mm^3 that is converted to 0.1µL or 10^{-4}ml).

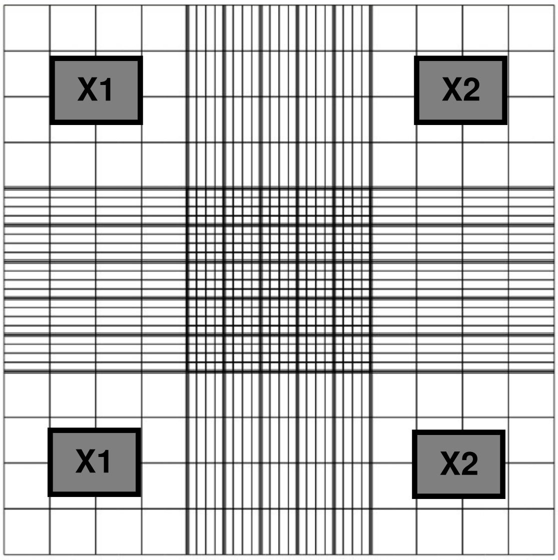

Figure 12 - Scheme of the Neubauer Chamber. Despite the fact of the recent technical development of scientific laboratories, the Neubauer chamber remains the most common method used for cell counting around the world.

2.1.2 Cell lines

For this study we used cell line derived from Human Embryonic Kidney (HEK) 293T cells and UACC-62 (a malignant melanoma cell line). Both provided by American Type Culture Collection (ATTC).

2.2 Western Blot

Western blotting is an important technique used in cell and molecular biology. It allows the identification of specific proteins from a complex mixture of proteins extracted from cells, based on protein separation according to their molecular weight [88].

2.2.1 Total protein extraction

To get access to the total protein extract present in the cells, we need to rupture the cytoplasmic cell membrane allowing all the intracellular components to be released.

Once the cell plates were confluent we washed the cells with 1x PBS and collected them. Next, we centrifuged cells at 1100 revolutions per minute (rpm) for 4 minutes and discarded the supernatant.

All the procedures below were performed on ice to preserve the integrity of the extracted proteins.

Protein extraction was made using CST buffer (1 M Tris pH 7.5 (Fisher Scientific, EUA), 5 M NaCl (Merck, Germany), 5% Triton X-100 (Amresco, Ohio), 1M NaF (VWR, EC), 0.5M EDTA (Sigma Aldrich, USA), 0.5M Ethylene glycol-bis-(β-aminoethyl ether)-N’,N’,N’,N’-tetraacetic acid (EGTA; AppliChem, Germany), 200mM Sodium Pyrophosphate (Santa Cruz, Dallas), 1M β-Glycerolphosphate(β-G-P; Santa Cruz, Dallas), 100mM sodium orthovanadate (OVO4; Sigma Aldrich, USA) 0.1 mg/µL Calyculin A (Santa Cruz, Dallas) and 0.1 mg/µL Protease Inhibitors Cocktail (PIC; Sigma Aldrich, USA)). We added the proper volume of CST to the cell pellet and homogenised the samples by pipetting up-and-down and a brief vortex. Next, we did a 20-minute incubation of the samples on an orbital shaker (Labnet, New Jersey) at 4 ºC. Then we centrifuged the samples at 15000 rpm (VWR, Japan) for 20 minutes at 4 ºC. Lastly, we transferred the supernatant (where the proteins were) to a new Eppendorf tube.

2.2.2 Total protein quantification

Most of the applications throughout this thesis require a rapid and accurate method to estimate protein concentration.

The amount of protein present in our samples was accessed using the Bradford (NZYTech, Portugal) method which is a very simple and fast technique based on a colorimetric shift of Comassie Brilliant Blue [89]. Moreover, the Bradford assay, has also low interference of other substances what makes it very sensitive [90]. By comparing the absorbances of our samples with the absorbances of a concentration known marker protein (for example Bovine Serum Albumine - BSA; ThermoFisher Scientific, USA) we can determine the protein concentration of our samples using a standard protein curve. The solutions used are represented in Figure 13.

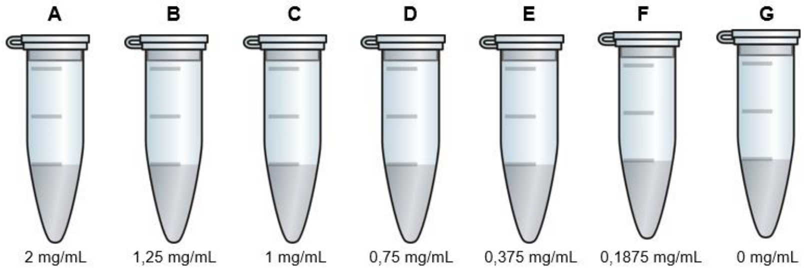

Figure 13 – BSA standard curve concentrations To determine the protein concentration of our test samples we used a linear standard curve. Serial dilutions were obtained from a BSA stock solution at 2000 µg/µL. Letters **A** to **G** refer to seven different BSA concentrations where A (2 mg/mL BSA), B (1.25 mg/mL BSA), C (0.75 mg/mL BSA), D (0.75 mg/mL), E (0.375 mg/Ml BSA), F (0.185 mg/mL BSA) and G (0 mg (mL BSA). All dilutions were obtained using H_2O

We diluted each of the test samples 1:10 (5 µL of sample in 45 µl of H_2O). Following, we loaded 5 µL of each test sample (1:10 dilution) and standard curve sample into a 96 well plate (in duplicated) and added 250 µL of Bradford to each well. The absorbance was measured on a microplate reader (Tecan Life Sciences, Austria) using I-control software. Using the absorbance and the linear standard curve: $y = mx + b$, where y=absorbance at 595 nm and x=protein concentration we calculated protein concentration for each of our test samples. Following, we normalized the protein concentration of all test samples using Laemmli 6x (0.2 M TrisHCl (Sigma Aldrich, USA), pH 6.8, 40% glycerol (Sigma Aldrich, USA), 0.04% Blue Bromophenol (Santa Cruz, Dallas), 0.3 M SDS (Applichem, Germany), 20% β-Mercaptoethanol (Sigma Aldrich, Steinheim)) and extraction buffer. Laemmli is a protein-loading buffer that allows the visualization of the samples during the run (due to the presence of Blue Bromophenol) and simultaneously increases sample density for proper loading (due to glycerol) allowing the migration across the gel. The SDS present in the Laemmli charges the samples negatively, so the proteins can migrate to the positive pole, being separated according to their size.

Lastly, we heated the samples at 95 ºC in a Thermo Shaker (BioSan) for 5 minutes. This step allowed for denaturation of the proteins so that they can migrate on the gel when applying an electric stimulus. Samples were immediately loaded on a gel or stored at -20 ºC.

2.2.3 SDS-PAGE

The proteins were separated according to their molecular weight, as represented in Figure 14, in a sodium dodecyl sulfate polyacrylamide gel electrophoresis (SDS-PAGE; 0.4 M Tris (Sigma Aldrich, USA) pH 8.8, 10% acrylamide (Fisher Bioreagents, USA), 0.1% SDS (Applichem, Germany), 0.1% Ammonium Persulfate (APS; Sigma Aldrich, USA), 0.15% Tetramethylethylenediamine (TEMED; Santa Cruz Biotechnology, Dallas)).

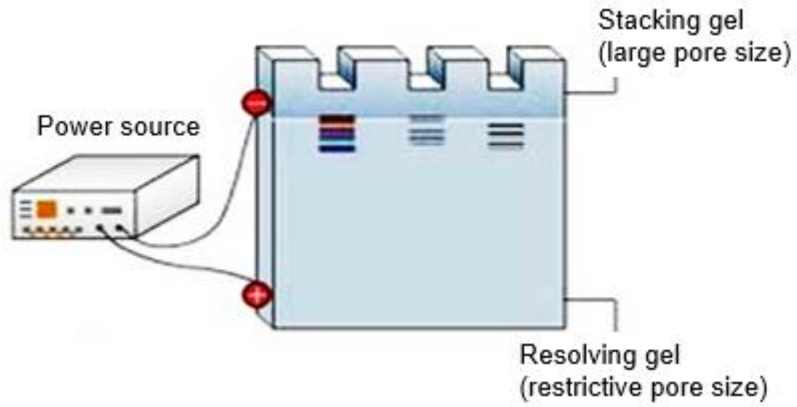

Figure 14 - Differently sized proteins migrate in different speeds across the gel. When the voltage is applied, the negative charged molecules migrate through the gel in direction to the positive pole. The small proteins in our samples migrate easily and the larger proteins are more likely to be retained (migrating less).

To obtain optimal protein resolution, we cast a stacking gel over the top of the running gel. This allows the proteins in a loaded well to be concentrated into one tight band during the first few minutes of electrophoresis before entering the running portion of the gel. The stacking gel was prepared with 0.1 M Tris (Sigma Aldrich, USA) pH 6.5, 3.8% acrylamide, 0.08% SDS, 0.1% APS, 0,1% TEMED. The stacking gel has large sized pores allowing proteins to migrate freely and get stacked at the interface between the stacking and the running gel. This allows for proteins to start migration at the same time.

The choice of the running gel percentage depends on the size of the protein of interest as it is shown in Figure 15.

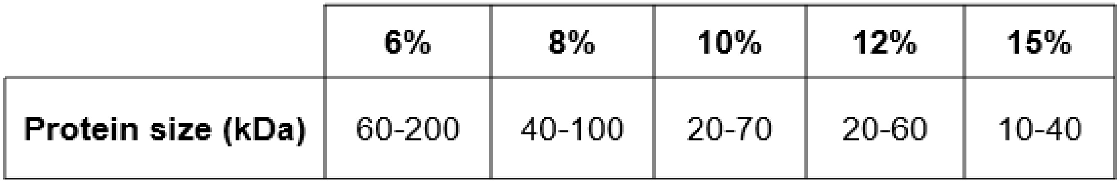

	6%	**8%**	**10%**	**12%**	**15%**
Protein size (kDa)	60-200	40-100	20-70	20-60	10-40

Figure 15 - Separation ranges of proteins in SDS-PAGE. The percentage of acrylamide present in the gel determine the speed of migration and the degree of separation between the proteins.

After loading the samples, the electrophoresis was performed in SDS-Page Running Buffer (0.02 M Tris (Sigma Aldrich, USA)), 0.025 M Glycine (Sigma Aldrich, Belgium), and 0.003 M SDS (Applichem, Germany)) using the BIO-RAD power source initially at 75 V until proteins enter the running gel and then at 150 V.

2.2.4 Protein transfer

After electrophoresis, the separated proteins present in the gel were transferred to a nitrocellulose membrane (Amersham, UK). The SDS-Page Transfer Buffer used contained 20% methanol (VWR, France), 0.05M Tris (Sigma Aldrich, USA) and 0.05% Glycine (Sigma Aldrich, Belgium). The transference was made using the BIO-RAD WB power source at 75 V for 90 minutes.

2.2.5 Blocking step

The blocking step is important to prevent the antibodies to bind to unspecific proteins existing in the membrane surface.

As blocking reagents, we used 5% BSA (Thermo Scientific, USA) or 5% Milk (Nestlé, Portugal). The proteins present in these solutions blocked the unoccupied sites on the membrane thus reducing background at detection time and improving the signal-to-noise ratio of the assay. This incubation was made at room temperature for 1 hour with agitation.

2.2.6 Antibodies incubation

After blocking, the membrane was incubated overnight at 4 ºC using a roller mixer (Stuart, UK) with a primary antibody that binds to the target protein, as shown in Table 1.

Table 1 - List of the information about the antibodies used in this project

Antibody	Species	Dilution	Company	#Catalog
TRIB2	Rabbit	1:800	Cell Signaling Technology	13533S
p-AKT 473	Rabbit	1:500	Santa Cruz Biotechnology	sc-7985-r
p-AKT 308	Rabbit	1:1000	Cell Signaling Technology	4056S
t-AKT	Rabbit	1:1000	Cell Signaling Technology	9272S
HA	Mouse	1:1000	Cell Signaling Technology	2367S
MYC	Mouse	1:1000	Santa Cruz Biotechnology	sc-47694
GAPDH	Rabbit	1:5000	Santa Cruz Biotechnology	sc-25778
Anti-rabbit	Donkey	1:10000	GE Healthcare Life Sciences	NA931V
Anti-mouse	Sheep	1:1000	GE Healthcare Life Sciences	NA934V
Anti-mouse Light Chain Specific	Mouse	1:1000	Cell Signaling Technology	58802S

The following day, the membranes were washed to remove residual unbound primary antibody, with TBS-Tween (0.075 M Tris (Sigma Aldrich, USA), 0.15 M NaCl (Merck Millipore, Germany), 0.1% Tween 20 (Merck Millipore, EC) for three times, about 5 minutes each with agitation. We then incubated with the second antibody for 1 hour, at room temperature, with agitation. This step allows for the first antibody to be recognized and detected. The membrane was then washed with TBS-Tween for three times, 5 minutes each, with agitation.

2.2.7 Protein detection

This step allows the detection of the localized probe to document the position and the relative abundance of the target protein.

The membrane was incubated for 5 minutes in an enhanced chemiluminescence (ECL; 1.25 mM Luminol (Sigma Aldrich, USA) diluted in DMSO, 0.2 mM p-coumaric acid (Sigma Aldrich, UK) diluted in DMSO, 0.1 M Tris pH 8.5, 0.01% H_2O_2 (VWR, EC)). The enzyme HRP (horseradish peroxidase) coupled to the secondary antibody luminol is oxidized, in the presence of peroxide, producing and excited state product that emits luminescence.

The signal was detected using the software Image Lab 4.0 of Chemidoc (Bio-Rad, USA).

2.3 Protein Complementation Assay

.Protein Complementation Assay (PCA) system has been suggested to be one of the most useful tools among the other methods to study protein-protein interaction [91]. This system is based on interaction-driven reconstitution of the activity of a reporter protein (luciferase, in this case) that is split into two fragments as represented on Figure 16.

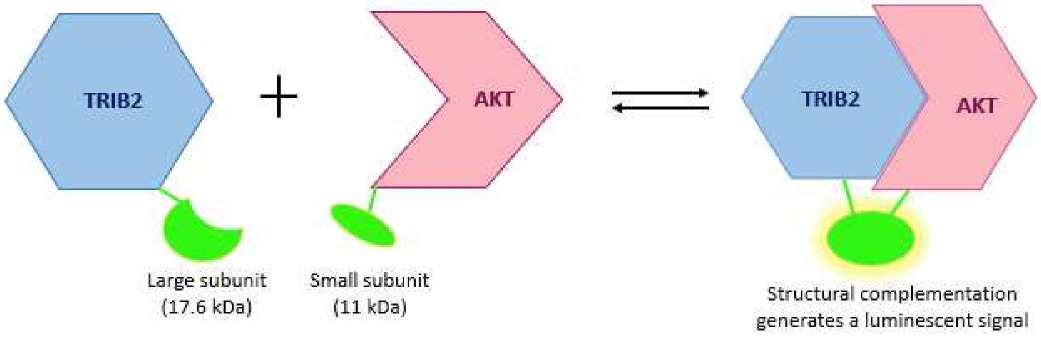

Figure 16 - Scheme of the PCA structural associations. PCA is a structural complementation assay designed for PPIs studies. The system is composed of two subunits, Large BiT (LgBiT; 18kDa) and Small BiT (SmBiT; 11 amino acid peptide) that are expressed as fusions to target proteins of interest. If these two proteins do interact the split fragment of luciferase will come together and give off a luminescence signal in the presence of an added substrate Promega Nano-Glo Live Cell Assay system (#N2011).

We plated 293T cells at a density of 25 000 per 100 µL of standard cell culture media in a 96 well plate. We used triplicates for each condition. Cells were maintained in standard cell culture incubation for 24 hours.

The next day, each well was transfected with a total of 100 ng or 150 ng of plasmid DNA. We mixed plasmids and top up to 10 µL with serum-free medium. We added 2 µL of Fugene6 transfection reagent (Promega #E2691) for each well to be transfected. Then we replaced old medium with the transfection mixture and incubated for 24 hours at 37 ºC. Next we performed a luciferase assay using Promega Nano-Glo Live Cell Assay system (#N2011). Briefly, we discarded the medium and carefully washed once with 1x PBS. Added 25 µL of 1x PBS to detach all the cells and transferred them to a non-transparent white 96 well plate (we left a gap for each condition to avoid signal spillage). We added 25 µL of the luciferase reagent to each well and incubated at room temperature for 5 minutes. We acquired the luminescence reading on microplate reader (Tecan Life Sciences, Austria) using the I-control software.

The data analysis was done using Microsoft Office Excel.

2.4 PCA Optimization

Every protein of interest could be linked to the Small or the Large luciferase fragment in its amino or carboxyl termination, so it is crucial to optimize the PCA system in order to obtain the best luminescence signal. The optimization was done by testing every possible combination of these constructs, represented on Figure 17.

All of the constructs used in the PCA were a kind gift from our collaborator Dr.Endre Kiss-Tooth from the University of Sheffield. The results from the optimization step are described in the section of the Results.

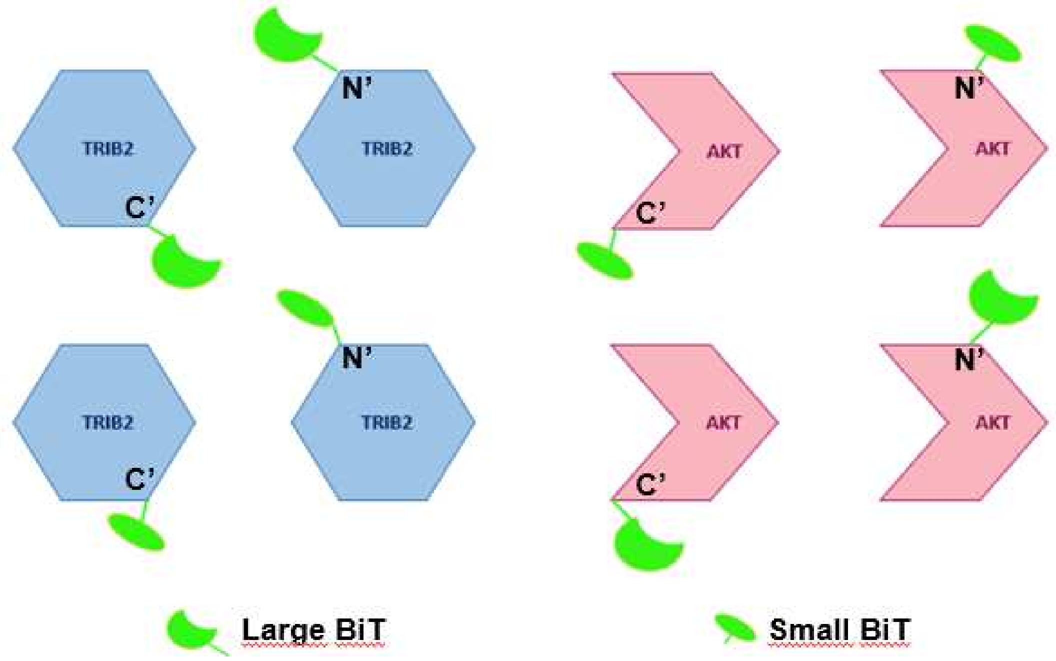

Figure 17 - Possible constructs of TRIB2 and AKT. There are four possible fusions of the protein of interest to the luciferase fragment. Each protein of interest can be cloned next to a Small or Large luciferase fragment or fused to either its C' or N' terminal region.

2.5 Plasmid amplification

The process of plasmid amplification is normally used to replicate or clone plasmids for future applications as transfections. Because of this, nearly all plasmids carry both a bacterial origin of replication and an antibiotic resistance gene for use as a selectable marker in bacteria.

2.5.1 Bacterial transformation and plasmid amplification

Transformation is the process by which foreign DNA is introduced into a cell, in this case, into bacteria. We used the DH5 alpha *E. Coli* Strain of bacteria that were stored at -80 ºC. We added 1 µL of DNA to 25 µL of bacteria, mixed the tube gently and incubated 30 minutes on ice. Following, the mixture was incubated on a 42 ºC water bath for 45 seconds and placed back on ice. Next, we added 400 µL of Liquid SOC Medium (NZYTech, Portugal) rich in glucose to induce bacteria growing. We incubated the tube for one-hour on a 37 ºC shaking incubator (Thrmomixer compact, Eppendorf). Then, we resuspend the pellet and plated onto a 10cm LB Agar (NZYTech, Portugal) plate containing the appropriate antibiotic. We incubated the plates at 37 ºC overnight.

The next day we picked one colony of the plate using a pipet tip and grew on 50 mL of LB Medium with the proper antibiotic. Next, we incubated the solution overnight, at 37 ºC and orbital shaking.

2.5.2 DNA extraction

After 12/14 hours we extracted the DNA extraction using a Midi Prep Kit (VWR, USA). We followed manufactures instructions according to Annex A.

2.6 Immunoprecipitation

Immunoprecipitation is a method of isolating a specific protein from a complex mixture such as a cell lysate. The basic principle is very simple: the protein of interest is ‘captured’ by an antibody and then the protein-antigen complex is pulled out of the sample by the attachment to a bead. This protocol is used to study protein-protein interactions.

For the immunoprecipitation we used the Anti-Flag M2 Affinity Gel (Sigma Aldrich). We used 20 µl of bead slurry per sample. The beads were washed three times with CST buffer and the supernatant was carefully removed. We performed a blocking step by incubating the beads with a 5% BSA solution for 30 minutes at room temperature with gentle agitation. We washed the beads three times with CST buffer and the final bead volume was adjusted with CST buffer. We added 20 µL of bead slurry to each sample and incubated the eppendorf tubes for 3 hours at 4 ºC. We centrifuged the tubes for 30 seconds and carefully removed the supernatant. We repeated the washes for three times using CST.
Following, we added Laemmli 6x (0,2M TrisHCl (Sigma Aldrich, USA), pH 6.8, 40% glycerol (Sigma Aldrich, USA), 0.04% Blue Bromophenol (Santa Cruz, Dallas), 0.3 M SDS (Applichem, Germany), 20% β-Mercaptoethanol (Sigma Aldrich, Steinheim)) and extraction buffer CST. Samples were heated to 95 ºC for 5 minutes and run on an appropriate percentage SDS-gel.

2.7 TRIB KO - CRISPR

For TRIB2 abrogation we used CRISPR-Cas9 technique. It allows genome editing and is a highly specific and efficient technique. CRISPR-Cas9 is based on a small guide RNA (sgRNA) that defines the genome target location and Cas9, a nuclease that induces double strand breaks at a specific site in the genome. Protospacer adjacent motif (PAM) is a 2-6 base pairs immediately adjacent to DNA sequence targeted by Cas9, which is crucial to Cas9 to recognize the DNA sequence, bind and cleave it [92]. This method causes small non sense mutations into the reading frame of the target gene via Non Homologous End Joining (NHEJ), a mechanism of repair that joints the two broken ends together leading to insertions and deletions.

The CRISPR-Cas9 system targeting TRIB2 was previously designed, optimized and validated by Dr.Bibiana Ferreira. We plated the cells in 6-well plates the day before transfection. The next day, we transfected 2µg of plasmid coding for two different sgRNAs (gRNA #1 **guide sequence:** GTTGTCGTCTATAAGGTCCG **CGG** and **gRNA#2 guide sequence:** TCGAAGAGTTGTCGTCTATA **AGG)** and Cas9. We changed the media the following day and added puromycin two days after for 48h to select the cells that contained the plasmid. To get individual clones we trypsinized the cells and performed serial dilutions to allow single clones to grow individually. Clones were selected by washing the cells twice with 1x PBS and individually trypsinized and plated them in two 60mm plates: a) a plate was used to extract the protein and test the abrogation of the protein by western blot and b) was used to keep a frozen stock.

Results

3 Results

Considering that TRIB2 and TRIB3 have different roles in tumorigenesis by controlling oppositely the phosphorylation of the Ser473 on AKT: TRIB2 enhances p-AKT of the Ser473 while TRIB3 decreases the p-AKT Ser473 the aim of this project is to understand if TRIB2 and TRIB3 compete for AKT binding.

3.1 PCA optimization

To test our hypothesis we decided to use the Protein Complementation Assay (PCA) as the first method to examine the physical interactions between tribbles members and AKT. This strategy was developed and previously described by Michnick and colleagues [93, 94] and was validated by Dr Endre Kiss-Tooth, our collaborator at the University of Sheffield [87].

PCA is based on the interaction-driven reconstitution of the activity of luciferase that is split into two fragments (a small one, represented by 1.1 and a large one, represented by 2.1), each fragment fused to each of our proteins of interest (TRIB2 and AKT or TRIB3 and AKT) in its amino (N) or carboxyl (C) termination. Therefore, by using this approach, the interaction of proteins can be visualized in live cells. All the constructs used in PCA were a kind gift from Dr Endre Kiss-Tooth.

We previously knew from our collaborator that the best luminescence signal for the association of TRIB3 and AKT was obtained using the small fragment of luciferase fused to the C terminal of TRIB3 (1.1 C-TRIB3) and the large fragment of luciferase fused to the C terminal of AKT (2.1 C-AKT).

To determine which pair of TRIB2 and AKT constructs would give the best luminescence signal, we had to test every possible combination of these plasmids.

To this end, we used 293T cells since the basal expression levels of tribble members are very low. The level of expression of tribble members has already been evaluated previously by other colleges in our lab, both by western blot and real-time PCR. Both expression and protein levels were higher in in melanoma cells SK-MEL28, G361 and A375 than in non melanoma cells 293T and U2OS, as represented on Figure 18.

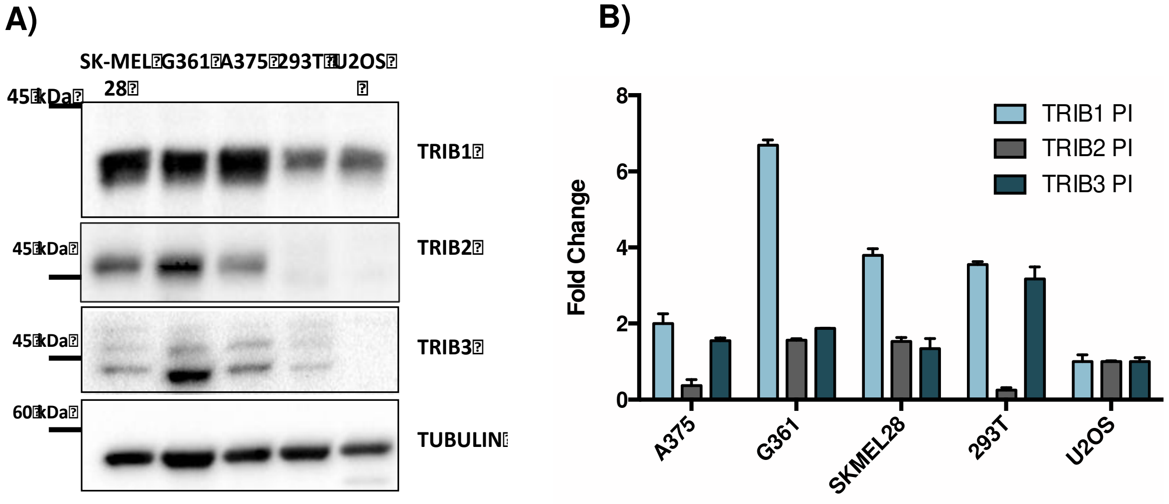

Figure 18 - **Presence of tribble members in melanoma and non-melanoma cell lines. A)** Western blot showing protein levels of Tribble family members in melanoma cell lines SK-MEL28, G361 and A375 and non-melanoma cell lines 293T and U2OS. Protein levels were assessed with Tribble specific antibodies. Tubulin was used as a loading control. 20 µg total protein loaded per lane and separated by 10% SDS-PAGE. **B)**. Tribble members (TRIB1, TRIB2 and TRIB3) mRNA levels of melanoma A375, G361 and SK-MEL28 and non melanoma cell lines 293T and U2OS. mRNA expression levels were evaluated using RT-PCR and data was analysed using Bio-Rad CFX manager 3.1 software.

In addition, 293T cells are easy to transfect. Cells were transfected with all the possible construct combinations and the luminescence signal was acquired. The combinations tested were the following:

1.1 N-TRIB3 x 2.1-N AKT
1.1 C-TRIB3 x 2.1 C-AKT
1.1 N-TRIB2 x 2.1-N AKT
2.1 C-TRIB2 x 1.1-N AKT
2.1 C-TRIB2 x 1.1 C-AKT
2.1 N-TRIB2 x 1.1-N AKT
2.1 N-TRIB2 x 1.1 C-AKT
1.1 N-TRIB2 x 2.1 C-AKT

The results in Figure 19 show that from all construct combinations the pairs 1.1 N-TRIB2 x 2.1 N-AKT and 1.1 N-TRIB2 x 2.1 C-AKT produced a significantly higher luminescence signal. These pairs were followed by 2.1 N-TRIB2 x 1.1 C-AKT, 2.1 C-TRIB2 x 1.1 N-AKT, 2.1 C-TRIB2 x 1.1 C-AKT and finally by 2.1 N-TRIB2 x 1.1 C-AKT.

The best luminescence signal was obtained using the small fragment of luciferase fused to the N terminal of TRIB2 (1.1 N-TRIB2) and the large fragment of luciferase fused to the N terminal of AKT (2.1 N-AKT).

Despite of having higher luminescence signal using the 1.1 C-TRIB23 x 2.1 C-AKT we chose to use the combination of TRIB3 and AKT that had the most similar signal to the pair of TRIB3 and AKT: 1.1 N-TRIB2 x 2.1 N AKT, highlighted with a red arrow in Figure 19. For this reason, the following experiments were performed using these two pairs of constructs:

1.1 N-TRIB3 x 2.1 N-AKT and 1.1 N-TRB2 x 2.1 N-AKT

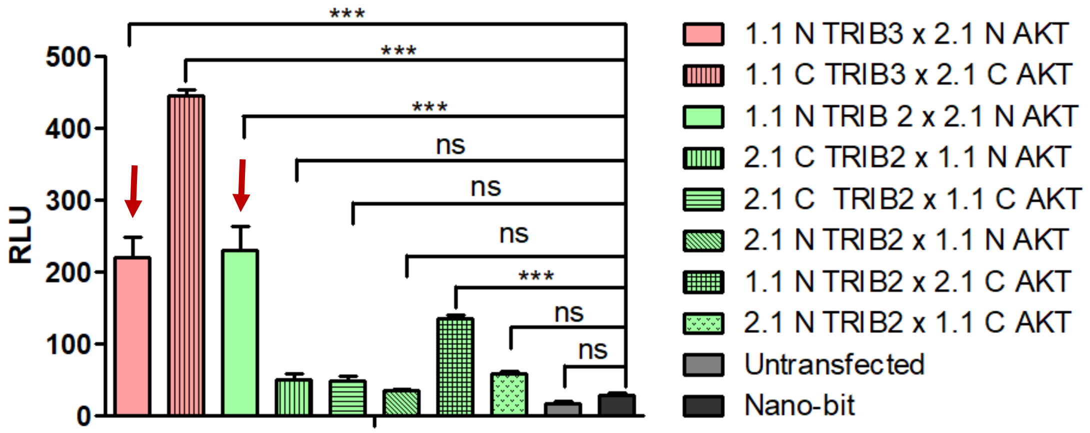

Figure 19 - PCA optimization. PCA is based on the interaction of two luciferase fragments, a small one (represented by 1.1) and a large one (represented by 2.1). Each one of these fragments can be fused to AKT or to TRIB2 in their amino (N) or carboxyl termination (C). We transiently transfected 293T cells for 24 hours using different pairs of constructs. At the end point we added the luciferase substrate for 5 minutes and acquired the luminescence signal. As negative control we used non-transfected cells (Untransfected) and cells transfected with an empty backbone (Nano-bit). RLU means Relative Luminescence Units. Data is represented as mean ± SEM; n = 3. P-values were obtained from Dunnett's Multiple Comparison Test; (***) P < 0.0001. ns means non-significant.

3.2 TRIB3 is able to disrupt TRIB2-AKT association

Our main goal was to test if TRIB2 and TRIB3 compete for AKT binding. In this sense we decided to analyse TRIB2-AKT association in the presence of increasing amounts of TRIB3 (from 10 ng to 50 ng). All transfections were performed with same amount of total DNA (150 ng) as represented in Table 2.

Table 2 - Amount of DNA transfected into 293T to analyse TRIB2 and AKT interaction in the presence of TRIB3. Cells were transfected with 50 ng of TRIB2 and 50 ng of AKT. The amount of TRIB3 varied from 0 to 50 ng. The empty backbone (Nano-bit) was transfected as the remaining amount to a total of 150 ng.

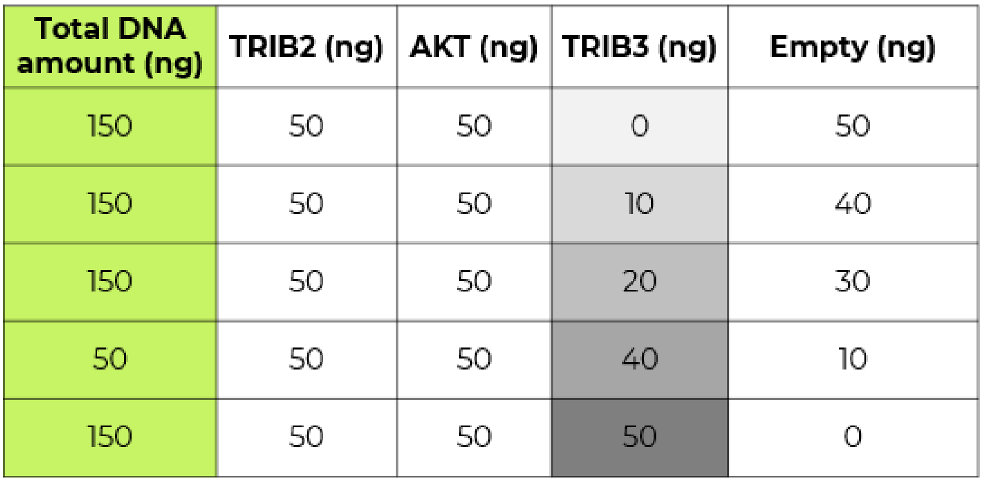

Total DNA amount (ng)	TRIB2 (ng)	AKT (ng)	TRIB3 (ng)	Empty (ng)
150	50	50	0	50
150	50	50	10	40
150	50	50	20	30
50	50	50	40	10
150	50	50	50	0

PCA results, represented in Figure 20, show that the luminescent signal decreased 45.2% in the presence of 40 ng and by 85% in the presence of 50 ng of TRIB3 (highlighted with a red arrow). These results are an indication that the strength of the TRIB2-AKT association is compromised by the increasing amounts of TRIB3. These data suggests that TRIB3 is able to disrupt the association between TRIB2 and AKT.

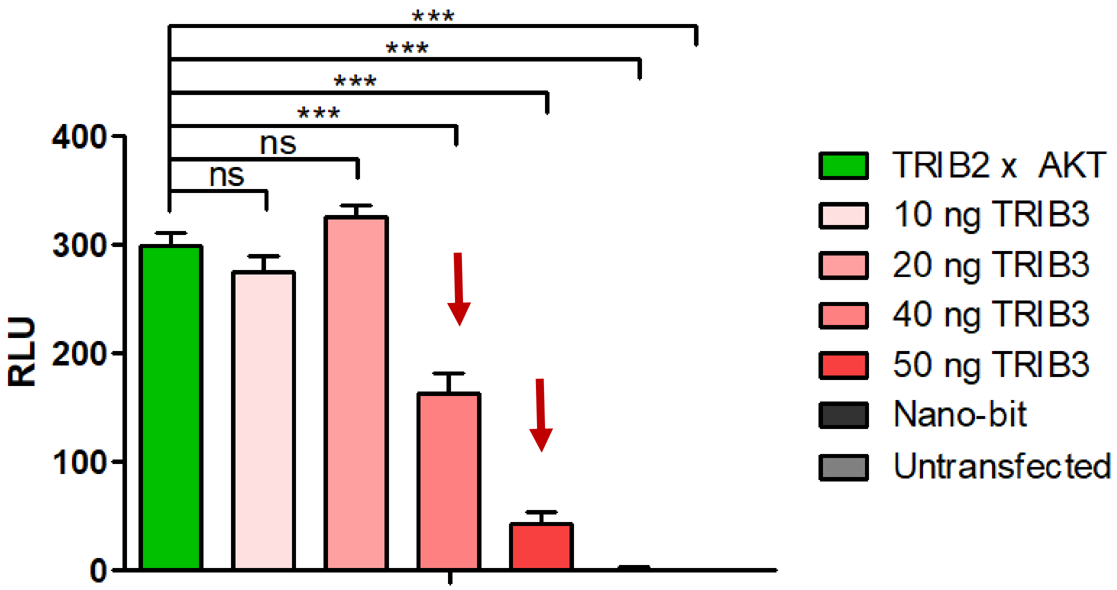

Figure 20 - The association between TRIB2 and AKT can be disrupted by TRIB3. We transiently transfected 293T cells with the indicated constructs for 24 hours. At the end point we added the luciferase substrate for 5 minutes and acquired the luminescence signal. As negative control we used non-transfected cells (Untransfected) and cells transfected with an empty backbone (Nano-bit). RLU means Relative Luminescence Units. Data is represented as mean ± SEM; n = 3. P-values were obtained from Dunnett's Multiple Comparison Test; (***) P < 0.0001. ns means non-significant.

3.3 TRIB2 stabilizes TRIB3-AKT interaction

To investigate if TRIB2 can disrupt TRIB3-AKT interaction, we decided to perform the opposite experiment, increasing the quantities of TRIB2 (from 10 ng to 50 ng) and analyse the dynamic interaction between TRIB3 and AKT using the PCA method.

Like in the previous experiment we transfected 293T cells with different constructs, always maintaining the total amount of DNA transfected (150 ng) as represented in Table 3.

Table 3 - Amount of DNA transfected into 293T cells to analyse TRIB3 and AKT interaction in the presence of TRIB2. 293T were transfected with 50 ng of TRIB3 and 50 ng of AKT. The amount of TRIB2 varied from 0 to 50 ng. The empty backbone (Nano-bit) was transfected as the remaining amount to a total of 150 ng.

Total DNA amount (ng)	TRIB3 (ng)	AKT (ng)	TRIB2 (ng)	Empty (ng)
150	50	50	0	50
150	50	50	10	40
150	50	50	20	30
50	50	50	40	10
150	50	50	50	0

Surprisingly, the results presented in Figure 21, show that there is a stronger association between TRIB2 and AKT in the presence of increasing amounts of TRIB3. The luminescent signal increased 75% with 20 ng and 109% with 40 ng TRIB2. In contrast, in the presence of 50 ng of TRIB2 the luminescent signal dropped almost to the level of the control in the absence of TRIB2.

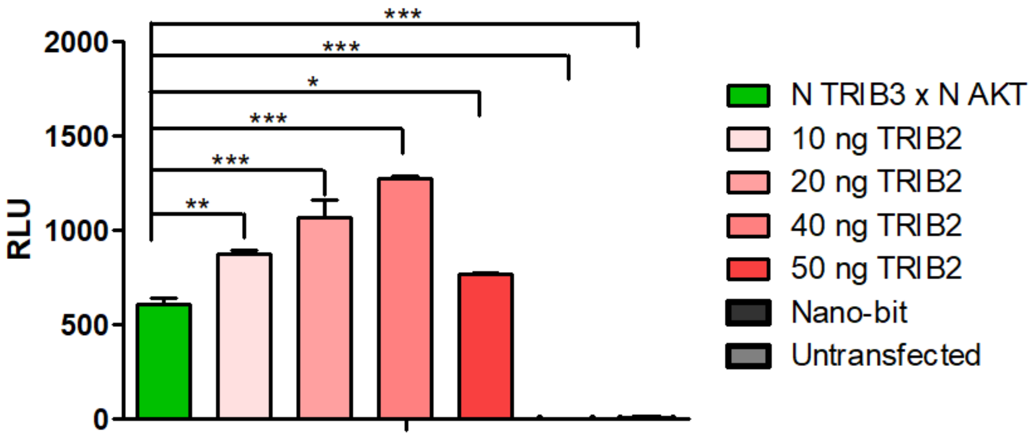

Figure 21 - The association between TRIB3 and AKT is stabilized by TRIB2. For this experiment we used 293T cell line. We did a 24h transiently transfection and acquired the luminesce 24 hours later, after 5 minutes exposure do luciferase substrate. As control we transfected only TRIB3 and AKT (absence of TRIB2), represented in the green bar. RLU means Relative Luminescence Units. Data are

represented as mean ± SEM; n = 3. P-values were obtained from Dunnett's Multiple Comparison Test; (***) $P < 0.0001$. ns means non-significant.

Taken together, the data obtained from the PCA experiments showed that TRIB3 is able to disrupt TRIB2 and AKT association. On the other hand, increasing amounts of TRIB2 do not seem to weaken TRIB3-AKT association. Moreover, TRIB2 seems to strengthen TRIB3 and AKT interaction. These experiments also showed that AKT preferentially binds TRIB3 over TRIB2.

Then we wanted to know **a)** if the disruption between TRIB2 and AKT in the presence of increasing amounts of TRIB3 would reflect a decrease in the phosphorylation of the Ser473 of AKT and **b)** if the stabilization of the association of TRIB3 and AKT caused by increasing amounts of TRIB2 would reflect a decrease in the AKT activation. To this end, we decided to analyse the AKT activation measuring the levels of phosphorylation of Ser 473 and Thr308. Note that the gel loading control was unequal and therefore the results, present in Figure 22, are not conclusive. We repeated the experiment on three different days and yet we did not achieve a reliable gel loading.

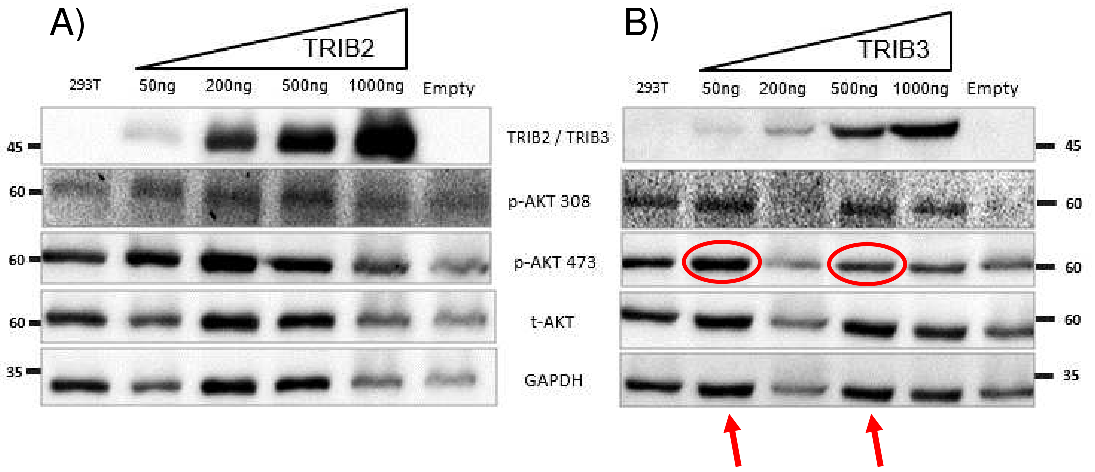

Figure 22 – Analysis of AKT activation. For this experiment we performed a 24h transient transfection in 293T cells of increasing amounts of TRIB2 (panel A) and increasing amounts of TRIB3 (panel B). As controls, we used the 293T parental cell line (represented as 293T) and 293T transfected with an empty backbone (represented as Empty). Cells were lysed and proteins were extracted. 40 µg of total protein was loaded per lane and separated by 10% SDS-PAGE. The protein levels were assessed by western blot using specific antibodies against TRIB2 and TRIB3 (represented on the first band on the left and right, respectively), p-AKT Thr308, p-AKT Ser473, total AKT (t-AKT) and GAPDH. GAPDH was used as a loading control.

The only two lanes that are comparable in panel in panel B are those resulting from transfection of 50 ng of TRIB3 and 500 ng of TRIB3, represented on Figure 22, labelled with a red arrow. In these two lanes it is visible that in the presence of 500 ng of TRIB3 there is less activation of AKT measured by the phosphorylation of Ser473, compared to cells with less TRIB3 (50 ng). These results also support the PCA data previously shown on Figure 20.

3.4 293T stable cell line expressing TRIB2

To overcome the recurrent problem with gel loading which we hypothesized to be caused by the large amount of different DNA transfected into these cells, we decided to use a stable expression system to limit the number of constructs to be transfected. We used a 293T cell line stably expressing TRIB2 to analyse the role of TRIB3 on AKT activation. Unlike the short-term protein expression observed during transient transfections, generating stable cell lines enables long-term protein expression studies. Moreover, repeating experiments in these cells as opposed to transiently-transfected cells increase reproducibility as it eliminates the variation associated with repeated transient transfections.

We transfected 293T cell line with a TRIB2 FLAG tagged plasmid and an empty vector plasmid. Figure 23 shows that this 293T cell line stably express TRIB2.

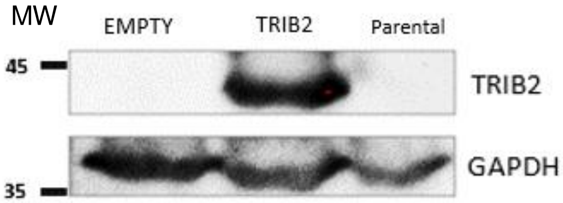

Figure 23 - 293T stable cell line expressing TRIB2. For this experiment we used 293T cell line. The stable transfection of TRIB2 enables the expression of TRIB2 on 293T cells that normally have none or low expression of this protein. As transfection controls we used the 293T parental cell line (represented as Parental) and cells transfected with an empty backbone (represented as EMPTY); 40 µg total protein loaded per lane and separated by 10% SDS-PAGE. Protein levels were assessed with the specific tribbles antibodies by western blot technique. GAPDH was used as a loading control. MW means molecular weight.

By using these stable cell lines for co-immunoprecipitation, we investigated if the strenght of the association between TRIB2 and AKT is compromised in the presence of TRIB3, as suggested by the data obtained by the PCA experiments. Co-immunoprecipitation is a technique widely used for the analysis and validation of protein-protein interactions.

We transiently transfected increasing amounts of TRIB3, from 50 ng to 1000 ng, together with 500 ng of AKT into 293T cells stably expressing TRIB2-FLAG or empty parental vector. The immunoprecipitation was performed using specific anti-FLAG M2 Sepharose Beads (TRIB2 tag). M2 is a mouse monoclonal antibody that recognizes the FLAG sequence at the N-terminus of TRIB2. This allows the detection and capture of fusion proteins containing a FLAG peptide sequence, as TRIB2.

The results are represented in Figure 24. By using a cell line that stably expresses TRIB2 allowed us to **a)** have all the experimental conditions expressing TRIB2 at the same level and **b)** reduce the amount of total DNA transfected into the cell.

The blots for the whole extract (WE) confirmed the presence of TRIB2 in the 293T cell line, the transient transfection of AKT and the increasing amounts of TRIB3. The blots showing the immunoprecipitated fraction shed doubt on the specificity of the beads used to precipitate TRIB2 since, in cell lysates where TRIB2 is not present as in lane 2 of the IP blot, a band corresponding to AKT and TRIB3 is clearly visible. In the absence of TRIB2, this result might be explained by a) a poor washing procedure leaving unspecific cell components stuck to the beads or b) unspecific binding properties of the beads. As washing was performed in a very stringent and established manner, unspecific binding to the beads seems to be a reasonable explanation.

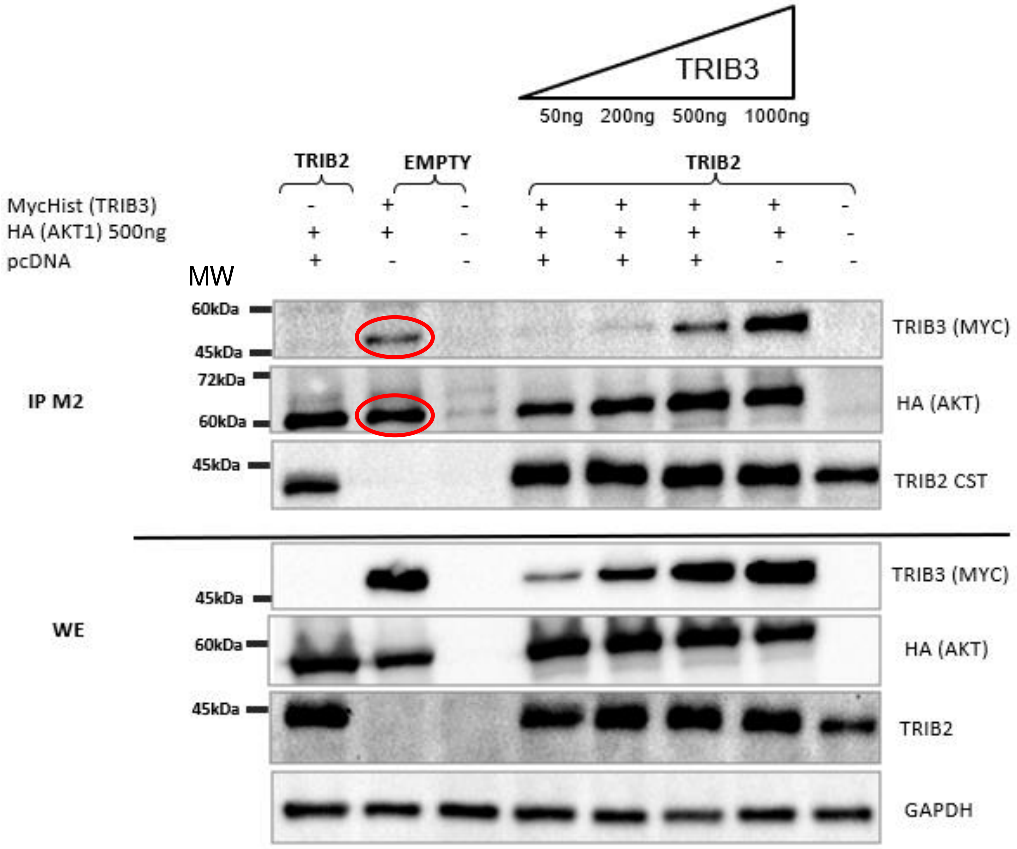
TRIB3
50ng
200ng
500ng
1000ng
TRIB2
EMPTY
TRIB2
MycHist (TRIB3)
HA (AKT1) 500ng
pcDNA
MW
60kDa
45kDa
72kDa
60kDa
45kDa
IP M2
TRIB3 (MYC)
HA (AKT)
TRIB2 CST
WE
45kDa
60kDa
45kDa
TRIB3 (MYC)
HA (AKT)
TRIB2
GAPDH

Figure 24 - Co-immunoprecipitation of FLAG to detect the association of TRIB2 to AKT in the presence of increasing amounts of TRIB3. Experiment done in 293T lysates from cells stable transfected with TRIB2. Cells transiently transfected with increasing amounts of TRIB3 (MycHist-tagged), 500 ng of AKT (HA-tagged) and the remaining amount until 1500 ng transfected with an empty backbone *(pcDNA).* The first three blots correspond to immunoprecipitated cell lysates with FLAG M2 beads (IP M2) and the last four blots correspond to the whole extract (WE) of cell lysates 40µg total protein loaded per lane and separated by 10% SDS-PAGE. Protein levels were assessed with the specific antibodies by western blot technique. GAPDH was used as a loading control. MW means molecular weight.

3.5 UACC-62: TRIB2 KO

For further experiments we will use a more representative system of melanoma, UACC-62 melanoma cell line to test our hypothesis that TRIB2 and TRIB3 compete for AKT binding. We need a system where TRIB2 and TRIB3 are normally expressed to study the consequences of TRIB2 abrogation. To generate such a cell system, we decided to abrogate TRIB2 expression using CRISPR-Cas9 technique, producing knock outs (KO). This technique allows highly specific and efficient genome editing. The CRISPR-Cas9 system targeting TRIB2 was previously designed and validated in our laboratory. 24 hours after plating the cells in 6-well plates, we transfected a plasmid coding simultaneously for single guide RNA (sgRNA) against TRIB2 and Cas9. Individual clones of TRIB2 KO containing the plasmid were selected using the antibiotic puromycin and tested through the analysis of protein expression by western blot using a specific antibody of TRIB2, as shown on Figure 25.

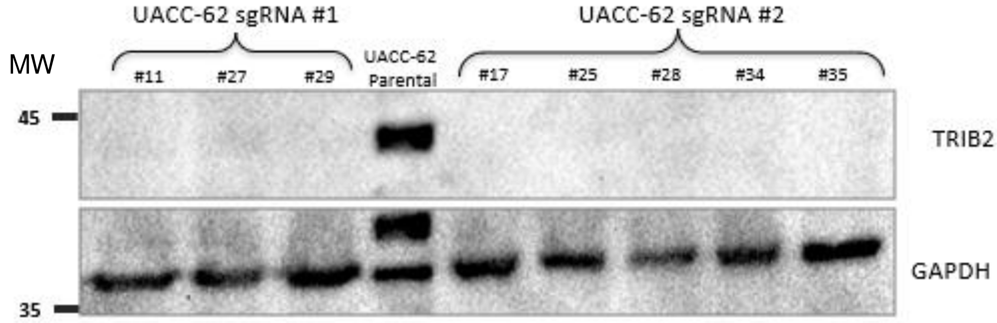

Figure 25 - TRIB2 KO UACC-62 cell line. The fourth lane shows UACC-62 parental cell line. The other lanes correspond to different clones for TRIB2 KO, using two different guide RNAs targeting two different sequences of aminoacids of TRIB2 protein. All the clones were positive KO for TRIB2. 40 µg total protein loaded per lane and separated by 10% SDS-PAGE. Protein levels were assessed with the specific antibodies by western blot technique. GAPDH was used as a loading control. MW means molecular weight.

In this cell line we obtained several TRIB2 KO with complete TRIB2 abrogation: #11, #27 and #29 (generated using sgRNA #1) and #17, #25, #28, #34 and #35 (using sgRNA #2). For further experiments we can use any of these clones.

Discussion

4 Discussion

Melanoma is the deadliest skin cancer. The majority of patients fail to respond to primary therapy or relapse within a year [95, 96]. Understanding the resistance mechanisms underlying melanoma resistance can be crucial to the development of new therapeutic approaches. Activation of AKT pathway is one of the most frequent events in melanoma, the phosphorylation of the Ser473 of AKT is correlated with poor clinical outcomes and resistance to melanoma treatment [21, 22, 24]. Based on the recent findings of our group that high TRIB2 protein levels were correlated with high AKT activation and taking into account the discoveries of our collaborators from Spain that TRIB3 seem to have the opposite effect on AKT, preventing its activation, **we hypothesized that TRIB2 and TRIB3 compete for AKT binding** [82, 85]**.**

To test the dynamic interaction between TRIB2 and TRIB3 with AKT we chose two independent approaches. We used the Protein Complementation Assay (PCA) and co-immunoprecipitation experiments. The first experiments using the PCA technique revealed that the best luminescence signal obtained for the association between TRIB3 and AKT was using the small fragment of luciferase fused to the C-terminal of TRIB3 (1.1 C TRIB3) and the large fragment of luciferase fused to the C-terminal of AKT (2.1 C AKT). These results are in agreement with previous findings from Dr.Endre Kiss-Tooth group showing that the N-terminal of TRIB1 and TRIB3, but not of TRIB2, appear to be responsible for the nuclear localisation of these proteins. Therefore, the fusion of the fragment of luciferase to the C-terminal domain of TRIB3 leaves its N-terminal ‘free’, contributing to maintain its function [97].

TRIB2 and TRIB3 association with AKT had the strongest signal using the small fragment of luciferase fused to the N-terminal of TRIB2 (1.1 N TRIB2) and the large fragment of luciferase fused to the N-terminal of AKT (2.1 N AKT). Dr.Endre’s group showed in previous studies that the C-terminal domain of TRIB2 may have unique functions as, unlike in other tribbles family members, its deletion leads to the exclusion of TRIB2/MAPKK complexes from the nucleus [97]. Therefore, leaving the C-terminal domain of TRIB2 free from the luciferase fragment is crucial to maintain the association with other proteins from the MAPK signaling pathway. In fact, our experiments revealed that when we used the constructs where luciferase is fused to the C-terminal domain of TRIB2, the luminescent signal that measures TRIB2 and AKT association is very low. These findings are in line to what has been previously published [97].

We found that **TRIB3 is able to disrupt TRIB2 and AKT association**. Recently, it has been shown that tribbles proteins compete for MAPK binding, but our data shows for the first time that tribbles members may also compete for AKT binding [87]. Moreover, recent studies showed that TRIB3 has an important role in the suppression of the tumorigenic process by controlling the levels of AKT phosphorylation by mTORC2 [79, 98]. Our findings suggest that the tumor suppressive activity of TRIB3 relies on its ability to disrupt the association between TRIB2 and AKT thus inhibiting the phosphorylation of the serine 473 on AKT by mTORC2. This suggestion is in concordance with findings from Velasco's and colleagues that suggest that the loss of TRIB3 produces an increase in the phosphorylation of AKT, thus contributing to the malignant progression of melanoma [79]

Our data also showed that increasing amounts of **TRIB2 stabilize TRIB3-AKT interaction**. This result was unexpected and there are no reports in the literature about this reciprocal interaction. One possibility that might explain this observation refers to cells that express low levels of TRIB3 depend more on TRIB2 to enhance AKT activation. On the other hand, in a cellular system expressing high TRIB3 levels, TRIB3 preferentially interacts with AKT preventing its activation. These experiments also suggest that AKT has a higher binding affinity for TRIB3 rather than TRIB2.

Since high levels of TRIB2 induce Ser473 AKT phosphorylation [82], we sought to understand if the decrease in the strength of TRIB2 and AKT association caused by TRIB3 presence would also reflect a decrease in the Ser473 AKT phosphorylation. Simultaneously, we also checked if a stronger TRIB3-AKT association induced by increasing levels of TRIB2 modulated AKT phosphorylation status.

Unfortunately, our results were not conclusive. The gel loading control was unequal probably due to the large amount of different DNAs transfected into 293T cells.

Despite these technical problems, the comparable lanes showed that cells transfected with more TRIB3 have less AKT activation. These results support our PCA data and suggest, once again, that TRIB3 is able to disrupt TRIB2-AKT interaction. Moreover, disturbing this protein complex results in less AKT activation and reinforces TRIB3 role as a tumor suppressor as it has been previously reported [98].

To overcome this technical problem, we used a **293T cell line stably expressing TRIB2,** previously generated in our lab by Dr.Bibiana Ferreira**.** Hence, the total amount of DNA to be transfected can be reduced and the levels of TRIB2 expressed are normalized in all experimental conditions. We have tried to validate the PCA results by analysing TRIB2-AKT association in the presence of TRIB3 using co-immunoprecipitation technique. The blots of the immunoprecipitated lysates were not conclusive and suggest that the beads used were not specific for TRIB2 in these cell line.

TRIB2 KO was performed in UACC-62 melanoma cell line, since it has high endogenous TRIB2 levels. We successfully abrogate TRIB2 and these cells will be used for following experiments regarding this topic

Conclusion

5 Conclusion and Future Perspectives

Melanoma is the deadliest form of skin cancer, being responsible for 80% of skin cancer deaths [99]. The identification and characterization of the principal pathways involved in melanoma progression is key to develop new and better therapies. Genetic analysis show that there are two frequently mutated signaling pathways in melanoma: MAPK pathway and PI3K/AKT pathway [21, 100]. The activation of PI3K/AKT pathway is one of the most frequent events in cancer and it is correlated with poor clinical outcomes and resistance mechanisms to MAPK pathway inhibitors used for melanoma treatment [21, 22]. The Link lab has discovered a novel mechanism of drug resistance facilitated by the oncoprotein TRIB2 via its direct interaction with AKT and consequently, AKT activation.

TRIB3, another member of tribbles family, has been proposed to exert the opposite effect on AKT, acting as an inhibitor of the phosphorylation of AKT and suggesting TRIB3 as a tumor suppressor [98]. Taking this into account, this project established an effort to understand if TRIB2 and TRIB3 compete for AKT binding.

Our data suggests for the first time that tribbles members TRIB2 and TRIB3 compete for AKT binding. Moreover, we suggest that the tumor suppressive activity that has been related to TRIB3 relies on its ability to disrupt the association between TRIB2 and AKT thus inhibiting AKT activation. Further studies are needed to understand the exact mechanism by which TRIB3 affects TRIB2 and AKT interaction.

Our data also suggests that only in a system with low TRIB3 levels TRIB2 is able to bind and activate AKT. It proposes that AKT has a higher binding affinity for TRIB3 rather than TRIB2.

In summary, despite the advances in the field of melanoma treatment in the past few years, most melanoma patients will eventually relapse. It is fundamental to study the resistance mechanisms associated with the administration of the current drugs for the development of better treatment options and strategies conceived for each patient.

TRIB2 was already suggested as a biomarker that predicts clinical responses to melanoma treatment [12]. Here, we show evidences that levels of TRIB3 should be maintained in cells to avoid TRIB2 oncogenic functions.

Future research may be focused on the exact molecular mechanism by which TRIB3 disrupts TRIB2 and AKT interaction. Hopefully, in the future the malignant consequences of high levels of TRIB2 expression in melanoma cells, may be counteracted by the oncossupressive protein TRIB3.

Bibliography

6 Bibliography

1. Eyers, P.A., K. Keeshan, and N. Kannan, *Tribbles in the 21st Century: The Evolving Roles of Tribbles Pseudokinases in Biology and Disease.* Trends Cell Biol, 2017. **27**(4): p. 284-298.
2. McCain, J., *The MAPK (ERK) Pathway: Investigational Combinations for the Treatment Of BRAF-Mutated Metastatic Melanoma.* P T, 2013. **38**(2): p. 96-108.
3. Glazer, A.M., et al., *Analysis of Trends in US Melanoma Incidence and Mortality.* JAMA Dermatol, 2016.
4. Hanahan, D. and R.A. Weinberg, *Hallmarks of cancer: the next generation.* Cell, 2011. **144**(5): p. 646-74.
5. Dickson, P.V. and J.E. Gershenwald, *Staging and prognosis of cutaneous melanoma.* Surg Oncol Clin N Am, 2011. **20**(1): p. 1-17.
6. Ferlay, J., et al., *Cancer incidence and mortality worldwide: sources, methods and major patterns in GLOBOCAN 2012.* Int J Cancer, 2015. **136**(5): p. E359-86.
7. Bray, F., et al., *Global cancer transitions according to the Human Development Index (2008-2030): a population-based study.* Lancet Oncol, 2012. **13**(8): p. 790-801.
8. Blanpain, C., *Tracing the cellular origin of cancer.* Nat Cell Biol, 2013. **15**(2): p. 126-34.
9. Vogelstein, B. and K.W. Kinzler, *Cancer genes and the pathways they control.* Nat Med, 2004. **10**(8): p. 789-99.
10. Friedberg, E.C., *DNA damage and repair.* Nature, 2003. **421**(6921): p. 436-40.
11. Hanahan, D. and R.A. Weinberg, *The hallmarks of cancer.* Cell, 2000. **100**(1): p. 57-70.
12. Hill, R., et al., *TRIB2 as a biomarker for diagnosis and progression of melanoma.* Carcinogenesis, 2015. **36**(4): p. 469-77.
13. Cichorek, M., et al., *Skin melanocytes: biology and development.* Postepy Dermatol Alergol, 2013. **30**(1): p. 30-41.
14. Houghton, A.N. and D. Polsky, *Focus on melanoma.* Cancer Cell, 2002. **2**(4): p. 275-8.
15. Yan, S., et al., *Epithelial-Mesenchymal Expression Phenotype of Primary Melanoma and Matched Metastases and Relationship with Overall Survival.* Anticancer Res, 2016. **36**(12): p. 6449-6456.
16. Tas, F., *Metastatic behavior in melanoma: timing, pattern, survival, and influencing factors.* J Oncol, 2012. **2012**: p. 647684.
17. Hussein, M.R., *Ultraviolet radiation and skin cancer: molecular mechanisms.* J Cutan Pathol, 2005. **32**(3): p. 191-205.
18. Pollock, P.M., et al., *High frequency of BRAF mutations in nevi.* Nat Genet, 2003. **33**(1): p. 19-20.
19. Patton, E.E., et al., *BRAF mutations are sufficient to promote nevi formation and cooperate with p53 in the genesis of melanoma.* Curr Biol, 2005. **15**(3): p. 249-54.
20. Villanueva, J., et al., *Acquired resistance to BRAF inhibitors mediated by a RAF kinase switch in melanoma can be overcome by cotargeting MEK and IGF-1R/PI3K.* Cancer Cell, 2010. **18**(6): p. 683-95.
21. Davies, M.A., *The role of the PI3K-AKT pathway in melanoma.* Cancer J, 2012. **18**(2): p. 142-7.
22. Yuan, T.L. and L.C. Cantley, *PI3K pathway alterations in cancer: variations on a theme.* Oncogene, 2008. **27**(41): p. 5497-510.
23. Dhillon, A.S., et al., *MAP kinase signalling pathways in cancer.* Oncogene, 2007. **26**(22): p. 3279-90.
24. Curtin, J.A., et al., *Distinct sets of genetic alterations in melanoma.* N Engl J Med, 2005. **353**(20): p. 2135-47.

25. Davies, M.A., *The multi-faceted roles of the PI3K-AKT pathway in melanoma.* Journal of Translational Medicine, 2015.
26. Slipicevic, A., et al., *Expression of activated Akt and PTEN in malignant melanomas: relationship with clinical outcome.* Am J Clin Pathol, 2005. **124**(4): p. 528-36.
27. Peng, W., et al., *Loss of PTEN Promotes Resistance to T Cell-Mediated Immunotherapy.* Cancer Discov, 2016. **6**(2): p. 202-16.
28. Morton, D.L., et al., *Validation of the accuracy of intraoperative lymphatic mapping and sentinel lymphadenectomy for early-stage melanoma: a multicenter trial. Multicenter Selective Lymphadenectomy Trial Group.* Ann Surg, 1999. **230**(4): p. 453-63; discussion 463-5.
29. Phan, G.Q., et al., *Sentinel lymph node biopsy for melanoma: indications and rationale.* Cancer Control, 2009. **16**(3): p. 234-9.
30. Morton, D.L., et al., *Final trial report of sentinel-node biopsy versus nodal observation in melanoma.* N Engl J Med, 2014. **370**(7): p. 599-609.
31. Perez-Herrero, E. and A. Fernandez-Medarde, *Advanced targeted therapies in cancer: Drug nanocarriers, the future of chemotherapy.* Eur J Pharm Biopharm, 2015. **93**: p. 52-79.
32. Crosby, T., et al., *Systemic treatments for metastatic cutaneous melanoma.* Cochrane Database Syst Rev, 2000(2): p. CD001215.
33. Yung, W.K., *Temozolomide in malignant gliomas.* Semin Oncol, 2000. **27**(3 Suppl 6): p. 27-34.
34. Agarwala, S.S., et al., *Temozolomide for the treatment of brain metastases associated with metastatic melanoma: a phase II study.* J Clin Oncol, 2004. **22**(11): p. 2101-7.
35. Sanada, M., et al., *Killing and mutagenic actions of dacarbazine, a chemotherapeutic alkylating agent, on human and mouse cells: effects of Mgmt and Mlh1 mutations.* DNA Repair (Amst), 2004. **3**(4): p. 413-20.
36. Damia, G. and M. D'Incalci, *Mechanisms of resistance to alkylating agents.* Cytotechnology, 1998. **27**(1-3): p. 165-73.
37. Johnson, D.B., C. Peng, and J.A. Sosman, *Nivolumab in melanoma: latest evidence and clinical potential.* Ther Adv Med Oncol, 2015. **7**(2): p. 97-106.
38. Alexandrov, L.B., et al., *Signatures of mutational processes in human cancer.* Nature, 2013. **500**(7463): p. 415-21.
39. Gaffen, S.L. and K.D. Liu, *Overview of interleukin-2 function, production and clinical applications.* Cytokine, 2004. **28**(3): p. 109-23.
40. Redman, J.M., G.T. Gibney, and M.B. Atkins, *Advances in immunotherapy for melanoma.* BMC Med, 2016. **14**: p. 20.
41. Ma, W., et al., *Current status and perspectives in translational biomarker research for PD-1/PD-L1 immune checkpoint blockade therapy.* J Hematol Oncol, 2016. **9**(1): p. 47.
42. Tarhini, A., E. Lo, and D.R. Minor, *Releasing the brake on the immune system: ipilimumab in melanoma and other tumors.* Cancer Biother Radiopharm, 2010. **25**(6): p. 601-13.
43. Margolin, K., et al., *Temozolomide and whole brain irradiation in melanoma metastatic to the brain: a phase II trial of the Cytokine Working Group.* J Cancer Res Clin Oncol, 2002. **128**(4): p. 214-8.
44. Meierjohann, S., *Crosstalk signaling in targeted melanoma therapy.* Cancer Metastasis Rev, 2017. **36**(1): p. 23-33.
45. Jenkins, R.W., D.A. Barbie, and K.T. Flaherty, *Mechanisms of resistance to immune checkpoint inhibitors.* Br J Cancer, 2018. **118**(1): p. 9-16.
46. Auslander, N., et al., *Robust prediction of response to immune checkpoint blockade therapy in metastatic melanoma.* Nat Med, 2018.
47. Brose, M.S., et al., *BRAF and RAS mutations in human lung cancer and melanoma.* Cancer Res, 2002. **62**(23): p. 6997-7000.

48. Chapman, P.B., et al., *Improved survival with vemurafenib in melanoma with BRAF V600E mutation.* N Engl J Med, 2011. **364**(26): p. 2507-16.
49. Bollag, G., et al., *Clinical efficacy of a RAF inhibitor needs broad target blockade in BRAF-mutant melanoma.* Nature, 2010. **467**(7315): p. 596-9.
50. Manzano, J.L., et al., *Resistant mechanisms to BRAF inhibitors in melanoma.* Ann Transl Med, 2016. **4**(12): p. 237.
51. Villanueva, J., A. Vultur, and M. Herlyn, *Resistance to BRAF inhibitors: unraveling mechanisms and future treatment options.* Cancer Res, 2011. **71**(23): p. 7137-40.
52. Liu, F., et al., *Targeting ERK, an Achilles' Heel of the MAPK pathway, in cancer therapy.* Acta Pharmaceutica Sinica B, 2018.
53. King, J.W. and P.D. Nathan, *Role of the MEK inhibitor trametinib in the treatment of metastatic melanoma.* Future Oncol, 2014. **10**(9): p. 1559-70.
54. Grimaldi, A.M., E. Simeone, and P.A. Ascierto, *The role of MEK inhibitors in the treatment of metastatic melanoma.* Curr Opin Oncol, 2014. **26**(2): p. 196-203.
55. Akinleye, A., et al., *MEK and the inhibitors: from bench to bedside.* J Hematol Oncol, 2013. **6**: p. 27.
56. Flaherty, K.T., et al., *Improved survival with MEK inhibition in BRAF-mutated melanoma.* N Engl J Med, 2012. **367**(2): p. 107-14.
57. Lim, S.Y., A.M. Menzies, and H. Rizos, *Mechanisms and strategies to overcome resistance to molecularly targeted therapy for melanoma.* Cancer, 2017. **123**(S11): p. 2118-2129.
58. Housman, G., et al., *Drug resistance in cancer: an overview.* Cancers (Basel), 2014. **6**(3): p. 1769-92.
59. Snyder, A., et al., *Genetic basis for clinical response to CTLA-4 blockade in melanoma.* N Engl J Med, 2014. **371**(23): p. 2189-2199.
60. Lito, P., N. Rosen, and D.B. Solit, *Tumor adaptation and resistance to RAF inhibitors.* Nat Med, 2013. **19**(11): p. 1401-9.
61. Welsh, S.J., et al., *Resistance to combination BRAF and MEK inhibition in metastatic melanoma: Where to next?* Eur J Cancer, 2016. **62**: p. 76-85.
62. Zahreddine, H. and K.L. Borden, *Mechanisms and insights into drug resistance in cancer.* Front Pharmacol, 2013. **4**: p. 28.
63. Michael, M. and M.M. Doherty, *Tumoral drug metabolism: overview and its implications for cancer therapy.* J Clin Oncol, 2005. **23**(1): p. 205-29.
64. Ortiz de Montellano, P.R., *Cytochrome P450-activated prodrugs.* Future Med Chem, 2013. **5**(2): p. 213-28.
65. Shen, H., et al., *Comparative metabolic capabilities and inhibitory profiles of CYP2D6.1, CYP2D6.10, and CYP2D6.17.* Drug Metab Dispos, 2007. **35**(8): p. 1292-300.
66. Borst, P. and R.O. Elferink, *Mammalian ABC transporters in health and disease.* Annu Rev Biochem, 2002. **71**: p. 537-92.
67. Szakacs, G., et al., *Predicting drug sensitivity and resistance: profiling ABC transporter genes in cancer cells.* Cancer Cell, 2004. **6**(2): p. 129-37.
68. Bonanno, L., A. Favaretto, and R. Rosell, *Platinum drugs and DNA repair mechanisms in lung cancer.* Anticancer Res, 2014. **34**(1): p. 493-501.
69. Selvakumaran, M., et al., *Enhanced cisplatin cytotoxicity by disturbing the nucleotide excision repair pathway in ovarian cancer cell lines.* Cancer Res, 2003. **63**(6): p. 1311-6.
70. Holohan, C., et al., *Cancer drug resistance: an evolving paradigm.* Nat Rev Cancer, 2013. **13**(10): p. 714-26.
71. Shang, Y., X. Cai, and D. Fan, *Roles of epithelial-mesenchymal transition in cancer drug resistance.* Curr Cancer Drug Targets, 2013. **13**(9): p. 915-29.
72. Mata, J., et al., *Tribbles coordinates mitosis and morphogenesis in Drosophila by regulating string/CDC25 proteolysis.* Cell, 2000. **101**(5): p. 511-22.

73. Seher, T.C. and M. Leptin, *Tribbles, a cell-cycle brake that coordinates proliferation and morphogenesis during Drosophila gastrulation.* Curr Biol, 2000. **10**(11): p. 623-9.
74. Bailey, F.P., et al., *The Tribbles 2 (TRB2) pseudokinase binds to ATP and autophosphorylates in a metal-independent manner.* Biochem J, 2015. **467**(1): p. 47-62.
75. Hegedus, Z., A. Czibula, and E. Kiss-Toth, *Tribbles: a family of kinase-like proteins with potent signalling regulatory function.* Cell Signal, 2007. **19**(2): p. 238-50.
76. Cunard, R., *Mammalian tribbles homologs at the crossroads of endoplasmic reticulum stress and Mammalian target of rapamycin pathways.* Scientifica (Cairo), 2013. **2013**: p. 750871.
77. Dedhia, P.H., et al., *Differential ability of Tribbles family members to promote degradation of C/EBPalpha and induce acute myelogenous leukemia.* Blood, 2010. **116**(8): p. 1321-8.
78. Dobens, L.L., Jr. and S. Bouyain, *Developmental roles of tribbles protein family members.* Dev Dyn, 2012. **241**(8): p. 1239-48.
79. Salazar, M., et al., *Loss of Tribbles pseudokinase-3 promotes Akt-driven tumorigenesis via FOXO inactivation.* Cell Death Differ, 2015. **22**(1): p. 131-44.
80. Zanella, F., et al., *Human TRIB2 is a repressor of FOXO that contributes to the malignant phenotype of melanoma cells.* Oncogene, 2010. **29**(20): p. 2973-82.
81. Lam, E.W., et al., *Forkhead box proteins: tuning forks for transcriptional harmony.* Nat Rev Cancer, 2013. **13**(7): p. 482-95.
82. Hill, R., et al., *TRIB2 confers resistance to anti-cancer therapy by activating the serine/threonine protein kinase AKT.* Nat Commun, 2017. **8**: p. 14687.
83. Oliner, J.D., et al., *Oncoprotein MDM2 conceals the activation domain of tumour suppressor p53.* Nature, 1993. **362**(6423): p. 857-60.
84. Freedman, D.A., L. Wu, and A.J. Levine, *Functions of the MDM2 oncoprotein.* Cell Mol Life Sci, 1999. **55**(1): p. 96-107.
85. Kiss-Toth, E., et al., *Human tribbles, a protein family controlling mitogen-activated protein kinase cascades.* J Biol Chem, 2004. **279**(41): p. 42703-8.
86. Du, K., et al., *TRB3: a tribbles homolog that inhibits Akt/PKB activation by insulin in liver.* Science, 2003. **300**(5625): p. 1574-7.
87. Guan, H., et al., *Competition between members of the tribbles pseudokinase protein family shapes their interactions with mitogen activated protein kinase pathways.* Sci Rep, 2016. **6**: p. 32667.
88. Mahmood, T. and P.C. Yang, *Western blot: technique, theory, and trouble shooting.* N Am J Med Sci, 2012. **4**(9): p. 429-34.
89. Bradford, M.M., *A rapid and sensitive method for the quantitation of microgram quantities of protein utilizing the principle of protein-dye binding.* Anal Biochem, 1976. **72**: p. 248-54.
90. Aminian, M., et al., *Mechanism of Coomassie Brilliant Blue G-250 binding to cetyltrimethylammonium bromide: an interference with the Bradford assay.* Anal Biochem, 2013. **434**(2): p. 287-91.
91. Drewes, G. and T. Bouwmeester, *Global approaches to protein-protein interactions.* Curr Opin Cell Biol, 2003. **15**(2): p. 199-205.
92. Ran, F.A., et al., *Genome engineering using the CRISPR-Cas9 system.* Nat Protoc, 2013. **8**(11): p. 2281-2308.
93. Remy, I. and S.W. Michnick, *Mapping biochemical networks with protein-fragment complementation assays.* Methods Mol Biol, 2004. **261**: p. 411-26.
94. Shi, R., et al., *[Analysis and verification of the interaction network of differentially expressed genes in invasive bladder cancer].* Nan Fang Yi Ke Da Xue Xue Bao, 2010. **30**(8): p. 1771-4.

95. Kulesa, P.M., J.A. Morrison, and C.M. Bailey, *The neural crest and cancer: a developmental spin on melanoma.* Cells Tissues Organs, 2013. **198**(1): p. 12-21.
96. Sun, C., et al., *Reversible and adaptive resistance to BRAF(V600E) inhibition in melanoma.* Nature, 2014. **508**(7494): p. 118-22.
97. Eder, K., et al., *Tribbles-2 is a novel regulator of inflammatory activation of monocytes.* Int Immunol, 2008. **20**(12): p. 1543-50.
98. Salazar, M., et al., *TRIB3 suppresses tumorigenesis by controlling mTORC2/AKT/FOXO signaling.* Mol Cell Oncol, 2015. **2**(3): p. e980134.
99. Cummins, D.L., et al., *Cutaneous malignant melanoma.* Mayo Clin Proc, 2006. **81**(4): p. 500-7.
100. Amaral, T., et al., *The mitogen-activated protein kinase pathway in melanoma part I - Activation and primary resistance mechanisms to BRAF inhibition.* Eur J Cancer, 2017. **73**: p. 85-92.

Annexes

Annex A

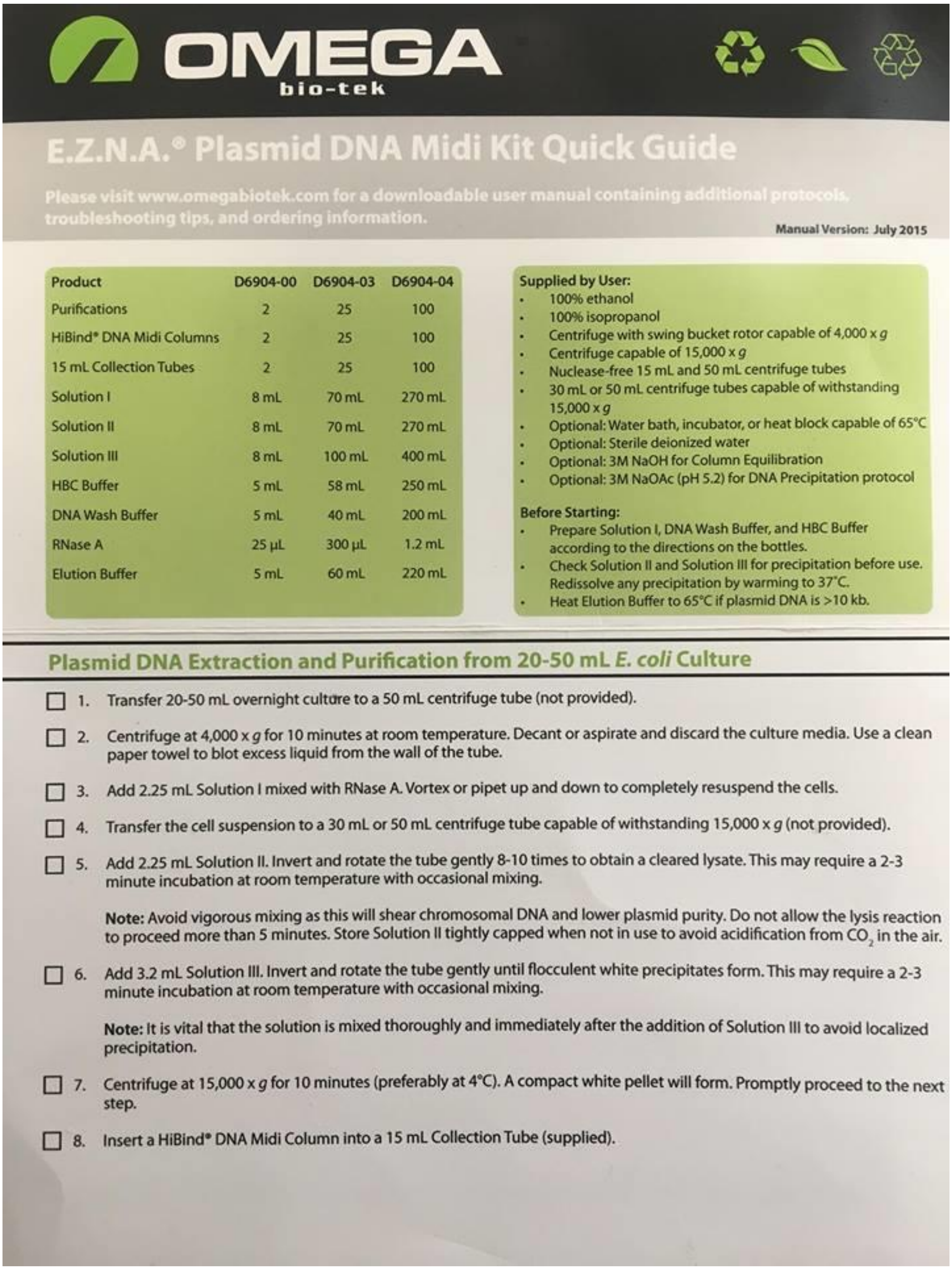

OMEGA bio-tek

E.Z.N.A.® Plasmid DNA Midi Kit Quick Guide

Please visit www.omegabiotek.com for a downloadable user manual containing additional protocols, troubleshooting tips, and ordering information.

Manual Version: July 2015

Product	D6904-00	D6904-03	D6904-04
Purifications	2	25	100
HiBind® DNA Midi Columns	2	25	100
15 mL Collection Tubes	2	25	100
Solution I	8 mL	70 mL	270 mL
Solution II	8 mL	70 mL	270 mL
Solution III	8 mL	100 mL	400 mL
HBC Buffer	5 mL	58 mL	250 mL
DNA Wash Buffer	5 mL	40 mL	200 mL
RNase A	25 µL	300 µL	1.2 mL
Elution Buffer	5 mL	60 mL	220 mL

Supplied by User:

- 100% ethanol
- 100% isopropanol
- Centrifuge with swing bucket rotor capable of 4,000 x *g*
- Centrifuge capable of 15,000 x *g*
- Nuclease-free 15 mL and 50 mL centrifuge tubes
- 30 mL or 50 mL centrifuge tubes capable of withstanding 15,000 x *g*
- Optional: Water bath, incubator, or heat block capable of 65°C
- Optional: Sterile deionized water
- Optional: 3M NaOH for Column Equilibration
- Optional: 3M NaOAc (pH 5.2) for DNA Precipitation protocol

Before Starting:

- Prepare Solution I, DNA Wash Buffer, and HBC Buffer according to the directions on the bottles.
- Check Solution II and Solution III for precipitation before use. Redissolve any precipitation by warming to 37°C.
- Heat Elution Buffer to 65°C if plasmid DNA is >10 kb.

Plasmid DNA Extraction and Purification from 20-50 mL *E. coli* Culture

☐ 1. Transfer 20-50 mL overnight culture to a 50 mL centrifuge tube (not provided).

☐ 2. Centrifuge at 4,000 x *g* for 10 minutes at room temperature. Decant or aspirate and discard the culture media. Use a clean paper towel to blot excess liquid from the wall of the tube.

☐ 3. Add 2.25 mL Solution I mixed with RNase A. Vortex or pipet up and down to completely resuspend the cells.

☐ 4. Transfer the cell suspension to a 30 mL or 50 mL centrifuge tube capable of withstanding 15,000 x *g* (not provided).

☐ 5. Add 2.25 mL Solution II. Invert and rotate the tube gently 8-10 times to obtain a cleared lysate. This may require a 2-3 minute incubation at room temperature with occasional mixing.

Note: Avoid vigorous mixing as this will shear chromosomal DNA and lower plasmid purity. Do not allow the lysis reaction to proceed more than 5 minutes. Store Solution II tightly capped when not in use to avoid acidification from CO_2 in the air.

☐ 6. Add 3.2 mL Solution III. Invert and rotate the tube gently until flocculent white precipitates form. This may require a 2-3 minute incubation at room temperature with occasional mixing.

Note: It is vital that the solution is mixed thoroughly and immediately after the addition of Solution III to avoid localized precipitation.

☐ 7. Centrifuge at 15,000 x *g* for 10 minutes (preferably at 4°C). A compact white pellet will form. Promptly proceed to the next step.

☐ 8. Insert a HiBind® DNA Midi Column into a 15 mL Collection Tube (supplied).

E.Z.N.A.® Plasmid DNA Midi Kit Quick Guide

☐ **OPTIONAL: Optional Protocol for Column Equilibration**

  ☐ 1. Add 1 mL 3M NaOH to the HiBind® DNA Midi Column.
  ☐ 2. Let sit at room temperature for 4 minutes.
  ☐ 3. Centrifuge at 4,000 x *g* for 3 minutes.
  ☐ 4. Discard the filtrate and reuse the collection tube.

☐ 9. CAREFULLY transfer 3.5 mL cleared supernatant from Step 7 to the HiBind® DNA Midi Column. Be careful not to disturb the pellet and that no cellular debris is transferred to the HiBind® DNA Midi Column.

☐ 10. Centrifuge at 4,000 x *g* for 3 minutes. Discard the filtrate and reuse the collection tube.

☐ 11. Repeat Steps 9-10 until all of the cleared supernatant has been transferred to the HiBind® DNA Midi Column.

☐ 12. Add 3 mL HBC Buffer diluted with 100% isopropanol (see the bottle for instructions). Centrifuge at 4,000 x *g* for 3 minutes. Discard the filtrate and reuse the collection tube.

☐ 13. Add 3.5 mL DNA Wash Buffer diluted with 100% ethanol (see the bottle for instructions). Centrifuge at 4,000 x *g* for 3 minutes. Discard the filtrate and reuse the collection tube.

☐ 14. Repeat Step 13 for a second DNA Wash Buffer wash step.

☐ 15. Centrifuge the empty HiBind® DNA Midi Column at 4,000 x *g* for 10 minutes to dry the column. This step is critical for removal of trace ethanol that may interfere with downstream applications.

☐ 16. Transfer the HiBind® DNA Midi Column to a nuclease-free 15 mL centrifuge tube (not supplied).

☐ 17. Add $\overset{0,3}{0.5}$-1 mL Elution Buffer or sterile deionized water directly to the center of the column matrix.

☐ 18. Let it sit at room temperature for 3 minutes.

☐ 19. Centrifuge at 4,000 x *g* for 5 minutes.

☐ 20. Store DNA at -20°C.

DNA Precipitation

The concentration of the eluted plasmid DNA varies with copy number, host strain, and growth conditions. In some cases, residual ethanol may also be present. To adjust the DNA concentration following plasmid DNA elution or for the removal of residual ethanol, perform the following isopropanol precipitation protocol.

☐ 1. Carefully transfer the eluted plasmid DNA to a clean tube suitable for precipitation. Add 1/10 volume 3M NaOAC (pH 5.2) and 0.7 volumes 100% isopropanol (room temperature). Vortex to mix.

☐ 2. Centrifuge at ≥15,000 x *g* for 20 minutes at 4°C. Carefully decant the supernatant.

☐ 3. Add 1-2 mL 70% ethanol. Vortex to resuspend the pellet.

☐ 4. Centrifuge at ≥15,000 x *g* for 10 minutes at 4°C. Carefully decant the supernatant.

☐ 5. Air dry the pellet for 10 minutes.

☐ 6. Add 200-500 µL Elution Buffer. Store DNA at -20°C.